DIAGNOSTIC AND PROGNOSTIC APPLICATION OF MOUNTAIN OBSERVATIONS

BY

J. BJERKNES
BERGEN

(Received July 23, 1924)

Preface.

The aim of dynamical meteorology is to make the meteorological science a branch of applied physics. The necessary base is a detailed meteorological diagnosis of the state of the atmosphere at a given moment. Then the physical equations give us a prognosis of the changes which will set in. All attempts which have been made to solve the problem of meteorological prognosis along this line have shown that our resources for meteorological diagnosis are still too incomplete. Where good networks of meteorological stations exist, a rather complete diagnosis is possible for the lowest layers of the atmosphere. But higher up, only sporadic and insufficient data are available.

The problem of meteorological diagnosis is, however, much simpler as soon as we restrict our attention to those atmospheric disturbances which in the first approximation may be assumed to pass without considerable change of structure. In this case the consecutive observations from one single station give a section through the passing phenomenon. The knowledge won by this method can again help us to reconstruct the three dimensional pictures of the same phenomenon at a given moment.

This method has recently been applied in two noteworthy papers, the one of Stüve, the other of Diesing. In the paper of Stüve*) aerological assents, which are made at relatively short intervals of time, are used for the construction of vertical sections through the passing atmospheric disturbances. These vertical sections show in a very instructive manner the position in space of the characteristic surfaces of discontinuity and their relation to clouds and precipitation. I shall often refer to Stüve's results later in this paper.

In the paper of Diesing**) the method of diagnosis is based on the use of registrations from mountain observatories. This method is of course confined to the layers below the level of 3 000—4 000 m., but for this part of the atmosphere it leads to a diagnosis

*) «Aerologische Untersuchungen zum Zwecke der Wetterdiagnose» (Die Arbeiten des Preussischen Aeronautischen Observatoriums. XIV. Band, 1922).

**) «Der Wärmeeinbruch (Warmfront) vom 12. bis 13. Januar 1920 in Mitteleuropa» (Veröffentlichungen des Geophysikalischen Instituts der Universität Leipzig. Band III, Heft I).

which is more complete than any aerological diagnosis made hitherto. Although the results of Diesing are based on the examination of one single case, they no doubt represent a valuable contribution to our knowledge of the atmospheric surfaces of discontinuity.*)

In the present paper I have used the same method of diagnosis as that of Diesing, viz:

To make a detailed diagnosis of the fields of mass and motion in the vicinity of an atmospheric surface of discontinuity, especially by utilizing the registrations from mountain observatories.

Basing on this diagnosis I have tried to arrive at a dynamical prognosis by aid of the equations of physics, viz:

From the obtained fields of mass and motion to deduce the fields of force which determine the fields of acceleration.

It will be seen later on that this programme can only be carried through under simplifying assumptions. Nevertheless, some laws of general validity can already be deduced from the results of this first attempt.

In the first descriptive part of the paper, which deals with the synoptic situation of the period in question, I have used the opportunity to bring in temperature registrations which show the typical difference of structure between newformed and old cyclones. Further, also to discuss some abnormalities in the structure of the cyclones due to the orographic influence of the Alps.

Thanks to the generosity of the Swiss Meteorological Institute, I have for a year had the opportunity of living in daily contact with the Alpine weather. On bringing forward the first results of the studies which I prepared during my stay in Zurich, I wish to express my heartiest thanks to the Swiss meteorologists for the excellent opportunity they gave me of profiting by the exceptionally favourable conditions of meteorological research in their country.

I. The Synoptic Situation 31st of Jan.—2nd of Feb., 1913**).

On the 31st of January (Fig. 1), a trough of low pressure extended from the North Sea down to the Alps. At first sight the front along the trough could be taken for a warm front. It had a zone of precipitation on its eastern side, and as a whole slightly higher temperatures behind than in front. However, the temperatures behind were not as high as they would be in a «tropical current» of that season, except perhaps at the stations of southern France. Furthermore, the rise of pressure directly after the passage of the front indicated that we had no warm front but a complex «occluded front» formed by the amalgamation of a warm and cold front. Until the evening of the same day (Fig. 1) the occlusion had reached Sweden—Eastern Germany—Austria and communicated with a shallow depression near Corsica.

In the morning of the 1st of February (Fig. 1), the occlusion had passed towards Russia, while in the Bay of Biscay a new disturbance appeared, which proved to be a rapidly moving young depression. In the evening (Fig. 1), it had reached the mouth of the Seine. The warm sector nearest to the centre did not have quite the temperature

*) Another paper, now in print in Veröffentlichungen des Geophysikalischen Instituts der Universität Leipzig: «Wellen und Wirbel an einer quasistationären Grenzfläche über Europa» by T. Bergeron and G. Swoboda, brings results which are in close relation to those of the present paper.

**) As to the terminology, I refer to the earlier papers of this publication: «Meteorological Conditions for the Formation of Rain», and «Life Cycle of Cyclones and the Polar Front Theory of Atmospheric Circulation».

which could be expected for a tropical current. On the Eiffel Tower, 335 metres above sea level, the temperature is, however, relatively higher and reaches 9°.5 just before the cold front arrived. This phenomenon must always appear when the depression moves, as in this case, faster than the surface air to the south of the track. Not before at the level of about 300 metres the warm sector air moves as fast or faster than the depression itself.

The next morning, 2nd of February (Fig. 1), the depression had arrived in the region of Hamburg. During the night it had deepened about 11 millibars, so that very steep pressure gradients and strong winds had arisen. The thermograms from Central Germany show a well marked warm period of a few hours in the morning of the 2nd of February. This must be due to the passage of a narrow warm sector, the remaining portion of which may be seen on the morning map, in the region of Magdeburg. In southern Germany, there are no surface temperatures which are correspondingly high to those over France the preceding day. We need, however, only to ascend some hundred metres above the plain in order to find real warm sector air. On Hohenpeissenberg (994 m.), we have thus at the morning observation + 5°.8, or more than two degrees warmer than in Munich (526 m.). Over Bohemia the air is considerably colder: Donnersberg (840 m.) — 1°.2 and Schneekoppe (1 610 m.) — 10°.3. The warm front surface is thus still to the west of these points.

In the course of the day the depression had its maximum depth and then gradually appeared less deep on the following maps (Fig. 1). The velocity had its maximum already during the night between the 1st and 2nd of February and decreased rapidly during the collapse of the depression over Russia.

Northern Italy remained cold during the entire passage of the depression. The warm attack from SW stopped at the Appenines and did not reach the Po valley before new cold air masses from France had begun a flanc attack which drove the warm air away towards the east. These attacks and counter attacks appear on the map as the formation of a secondary depression at the Riviera which afterwards moves away to the eastern part of the Mediterranean.

II. Temperature Variations at the Passage of the Occluded and the Newformed Depression.

Fig. 2. contains the temperature registrations of some stations at different levels in the region of the Alps during the passage of the two depressions described above.

When we first look at the registrations of Säntis (2 500 m.) and Belchen (1 394 m.) on the 31st, we find the course of the curves just as might be expected at the passage of an occluded cyclone. Säntis had a slight rise of temperature during the fall of pressure, then a sudden fall of temperature at the passage of the pressure trough itself. Belchen which is 1 100 metres lower had practically a constant temperature until the arrival of the trough line, then it had a fall of temperature. On Säntis we thus had a passage of an upper «warm sector» which had passed away above the level of Belchen.

The air in the rear of the occlusion proved to be much colder than that in front as well on Säntis as on Belchen. On the ground, however, the air mass behind the front is the warmest rather than the coldest part of the depression. This example shows that the temperatures at the ground may give perfectly false indications concerning the real temperature of air masses, and may disguise the phenomena of the free air. In our case

we have a «disguised cold wave»*) where the arriving air is of cold polar origin, but has been warmed from below, so that it has lost its character as a cold wave in the lowest layers.

Compared with the simple thermograms of Säntis and Belchen that of Zurich has quite a confusing embroidery of rapid rises and falls of temperature. In order to understand this curve we must take into account the conditions prevailing before the arrival of the occlusion. The region of the Alps was then in the southwestern border of an anticyclone (the same as that over Russia the 31st). The atmosphere was calm and had a rather stable stratification. Säntis had constantly about — 6° to — 5°, Belchen about 0°, and Zurich — 3° to 0°, which gives a lapse rate of about 0°.5/100 m. between Säntis and Belchen, and a temperature inversion below the level of Belchen. The strong SW winds arising in front of the depression on the morning of the 31st then swept away the cold surface layer and caused at $8^h.45$ a sudden rise of temperature from 1°.4 to 6°.1 in Zurich. Belchen, whieh from the beginning was above the cold surface layer had no rise of temperature in front of the trough. After the rise of temperature in Zurich, the lapse rate Zurich—Belchen was about 0°.7/100 m., or in other words, not much different from that between Belchen and Säntis.

The period of high temperature during the 31st in Zurich is, therefore, not due to a real «warm sector». It is merely an effect of the strong winds which made normal atmospheric conditions penetrate down to the ground.

The map of the 31st, 8^h shows that the rise of temperature registered in Zurich must have been a general phenomenon over a large area. Karlsruhe 7°.1 and Frankfort 5°.6 had had the same heating, whereas Munich — 2°.3 and Bamberg — 1°.2 were still within the cold surface layer. This thermal boundary was the intersection with the ground of the temperature inversion formed the preceding days in the anticyclone.

At the moment when the sudden rise of temperature occurred in Zurich the valleys of the Alps were still cold, and even at stations as Aarau and Basel to the west of Zurich (but at lower heights) some cold air had accidentally been left behind. Such cold air remainders passed Zurich later in the forenoon and caused the return of some short colder spells.

After the passage of the occluded front the temperature fell irregularly in different steps corresponding to the instability showers at the rear of the depression.

In the night between February 1st and 2nd during the passage of the next depression, Säntis, Belchen and Zurich all had a well marked period of high temperatures. Säntis during the 13 hours from 19^h the 1st to 8^h the 2nd, Belchen 12 hours from 18^h to 6^h, and Zurich 7 hours from midnight to 7^h (the preceding maximum at 14^h is of course due to the daily period). In this newformed deepening depression we thus find a warm sector at all levels — broad in the height and more narrow at the ground.

The high-level stations Zugspitze and Sonnblick, in the eastern part of the Alps, have temperature curves which in a general aspect are similar to that of Säntis — high temperature during the passage of the depressions and low temperatures between them.

Obir, which lies on the south side of the principal chain of the Alps, is not high enough to register the passage of the upper warm sector of the occlusion. The second cyclone, however, brought about a marked rise of temperature and a corresponding fall after the passage. The warm air arrives on Obir as a SW wind and has consequently passed over the cold air lake between the Alps and Appenines.

On Hohenpeissenberg, not far from Munich, one might have expected a similar thermogram to that of Belchen. The difference, however, is evident. At the first cyclone

*) The expression originates from H. Ficker who has discovered this phenomenon in his investigations of cold waves in the Alps. See for example «Der Transport kalter Luftmassen über die Zentralalpen», Denkschriften der Kaiserlichen Akademie der Wissenschaften, Vol. 80, p. 193.

passage where the warm sector passed away above the level of Belchen, a distinct rise of temperature was nevertheless recorded on Hohenpeissenberg although this mountain is 400 metres lower than Belchen. We here meet the influence of the foehn which is

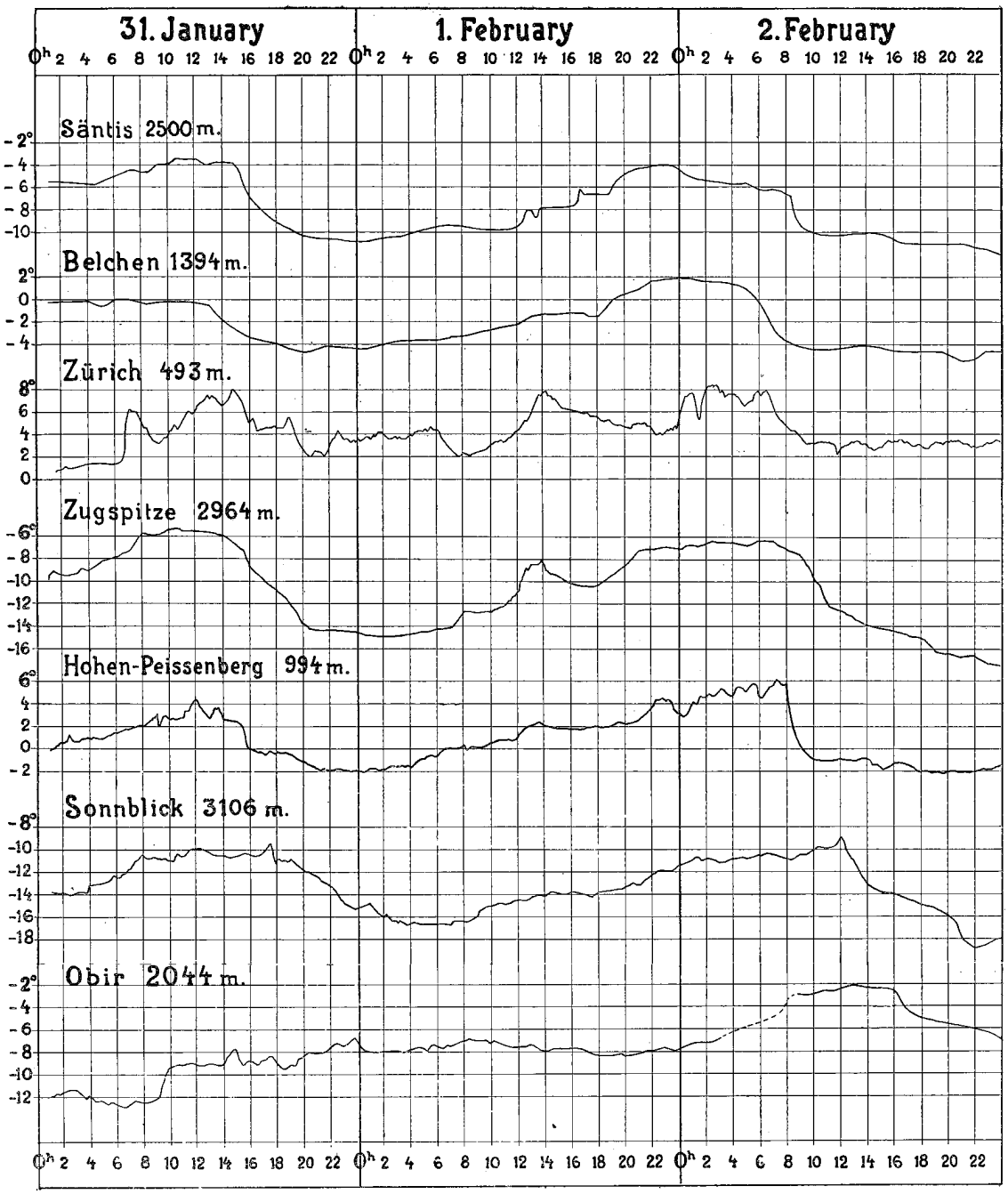

Fig. 2. Thermograms.

typical for the entire northern slope of the Alps and which brings about important modifications in the normal course of meteorological elements during the passage of cyclones. In our case, the occluded cyclone as well as the newformed one is characterized by a rise of temperature and a fall of relative humidity. Later when the winds turn from

South to a Western point, a fall of temperature and rise of relative humidity suddenly sets in. This termination of foehn is a real discontinuous phenomenon of the character of a cold front (or occlusion with the coldest air behind).

The warm fronts on the northern slope of the Alps do not usually appear with the same distinctness as the cold fronts. This can be seen on the Hohenpeissenberg thermogram at the passage of the newformed cyclone. The foehn which began at 22^h already brought so high temperatures before the arrival of the warm front that no decided rise of temperature occurred at the front passage itself. In our case the rise of temperature during the foehn phase is prob ably due to the arrival of warm sector air in the level from which the foehn originates.

The warm front precipitation undergoes corresponding degeneration. In our case Zugspitze had slight snowfall onwards from 21^h, but this precipitation must have evaporated when falling into the dry foehn current. On the lower stations the precipitation did not begin before the arrival of the cold front the morning of the 2nd.

When we abstract from the local phenomena such as surface inversions (in Zurich) and foehn influences (on Hohenpeissenberg), we see how the registrations of Fig. 2 give a good representation of the structure of the two cyclones in question — the occluded cyclone appears with an upper varm sector and colder air behind than in front, while the newformed cyclone appears with a warm sector at all levels. In one point, however, we must obviously make a reservation which has not been emphasized sufficiently in our earlier papers on the same subject — the boundary surfaces between the warm sector and its surroundings are in fact rather different from ideal surfaces of discontinuity. In some cases even, one finds an almost linear temperature change during several hours, so that we can no more point out the exact moment when the boundary surface did pass.

The best approximation to the mathematical discontinuity is found at the cold fronts — in our case as well as in most others. This quality has made the cold front phenomenon well known from the earliest period of meteorological science. The warm fronts are not so well known, so that a detailed description and dynamical analysis of this phenomenon might be of interest. For this purpose I have chosen the warm front of the new formed depression which passed Central Europe during the evening of the 1st of February.

III. Detailed Examination of the Warm Front Surface of the Newformed Cyclone.

a) Thermograms at Different Levels.

The registrations from Belchen, Säntis, Zugspitze and Sonnblick (Fig. 2) should be rather free from local disturbances (foehn, radiation etc.), and give the best approximation to the registration of an ideal instrument at a fixed point in the free atmosphere. The difference between the thermograms of these stations should, therefore, mainly be a function of the heights.

On Belchen, which is the lowest one, the position of the warm front surface is fairly well defined. There was a slight continuous rise of temperature during the day of the first, then from 16^h to 18^h a slight fall immediately followed by a brisk rise of temperature. It is most natural to fix the warm front passage to the time when the brisk rise began at 18^h.

On Säntis there is an analogous point of the registration at 19^h — after an almost horizontal curve, a sudden rise began which gradually passed into a slight rise persisting until 23^h. The Säntis thermogram had, however, also some other singular points which we did not find on Belchen. On Belchen we found a continuous rise of temperature

during the approach of the warm front, on Säntis we find the same rise, but it is subdivided into two great steps. The most conspicuous one is that at $16^h 3/4^h$.

As regards the Zugspitze thermogram one may hesitate as to the placing of the warm front. There is a distinct maximum at 14^h, then afterwards a minimum at 18^h, and again a linear rise lasting until 21^h. On consulting the humidities, we may, however, decide the question. The hourly values of relative humidity were:

until 13^h	14^h	15^h	16^h	17^h	18^h onwards
100	95	96	97	98	100 %

It seems most natural to explain the relatively dry period between 13^h and 18^h by a descending motion. This shows that the warm front surface must be placed at the second rise of temperature which began at 18^h.

Also on Sonnblick the thermogram alone is insufficient for the determination of the exact moment at which the warm front passed. On consulting the humidity, we find that the saturation began between 21^h and 22^h just at the moment when the temperature curve had its greatest inclination. The small hack in the thermogram at 21^h is therefore the most probable position of the warm front surface.

We have thus succeeded in determining the exact moments at which the warm front surface passed at the different mountain observatories: Belchen at 18^h, Säntis at 19^h, Zugspitze at 18^h, Sonnblick at 21^h. Further, we may state that the warm front was characterized by a sudden rise of temperature on the two lowest stations, Belchen and Säntis, whereas the «discontinuity» is almost effaced on Zugspitze and Sonnblick.

The sudden rise of temperature on Säntis at $12^h 3/4$ and $16^h 3/4$, and at Zugspitze at 13^h are probably due to the passage of another sort of inclined atmospheric boundary surfaces having drier air above than underneath. (The hygrogram of Zugspitze shows this. On Säntis the hygrograph has unfortunately not been in working order.) We have here, no doubt, to deal with the «Abgleitfläche» found by Stüve with the aerological observations from the observatory of Lindenberg.*)

The name «Abgleitfläche» alludes to a downward sliding motion on an inclined boundary surface, which in fact is the motion seen by an observer following the moving surface. The name has, however, the disadvantage that it might give the false impression of an actual countercurrent blowing downwards the «Abgleitfläche», thus in our case an easterly current. I would therefore prefer the name «surface of subsidence» and allow myself to use it in this paper. This name tells that the cold air subsides or in other words dilates horizontally and shrinks vertically (German: Schrumpfungsfläche).

b. Topography of the Warm Front Surface.

In the evening of the 1st of February the warm front surface was just in the region where the Swiss network of stations allowed a good determination of the surface topography (Fig. 3).

The warm front on the ground had just passed Besançon (311 m.) where the temperature was 7°.3 at 16^h, 10°.0 at 19^h and 11°.3 at 22^h. Mulhouse with 5°.4 still belongs to the cold air region, likewise all Swiss stations in the plain. La Chaux de Fonds (986 m.) on the western slope of Jura has a relatively high temperature compared to the other Jura stations. We may from this conclude that the warm front has at the moment to which the map refers, just got in touch with the ridge of the Jura. The pass

*) A very good description of the process of subsiding in a wedge of cold air has been given by M. A. Giblett in: «Upper Air Conditions after a Line-Squall» (Nature Dec. 15, 1923, p. 863).

stations St. Bernard (2 476 m.), St. Gotthard (2 103 m.) and Bernhardin (2 073 m.) give interesting indications concerning the position of the warm front surface at a higher level. St. Bernard had — 4°.2 whereas St. Gotthard and Bernhardin farther east had respectively — 7°.7 and — 8°.4. Bernhardin was below the warm front clouds (cloudy), St. Gotthard was in the same clouds (fog), and St. Bernard was above them (cloudless). At the same time Zermatt (1 610 m.) and Sierre (552 m.), not far from St. Bernard, had overcast, Sierre even slight rainfall. The wind direction on the St. Bernard, SW, proved that the warm air had passed south of the Mt. Blanc massif, in other words that the

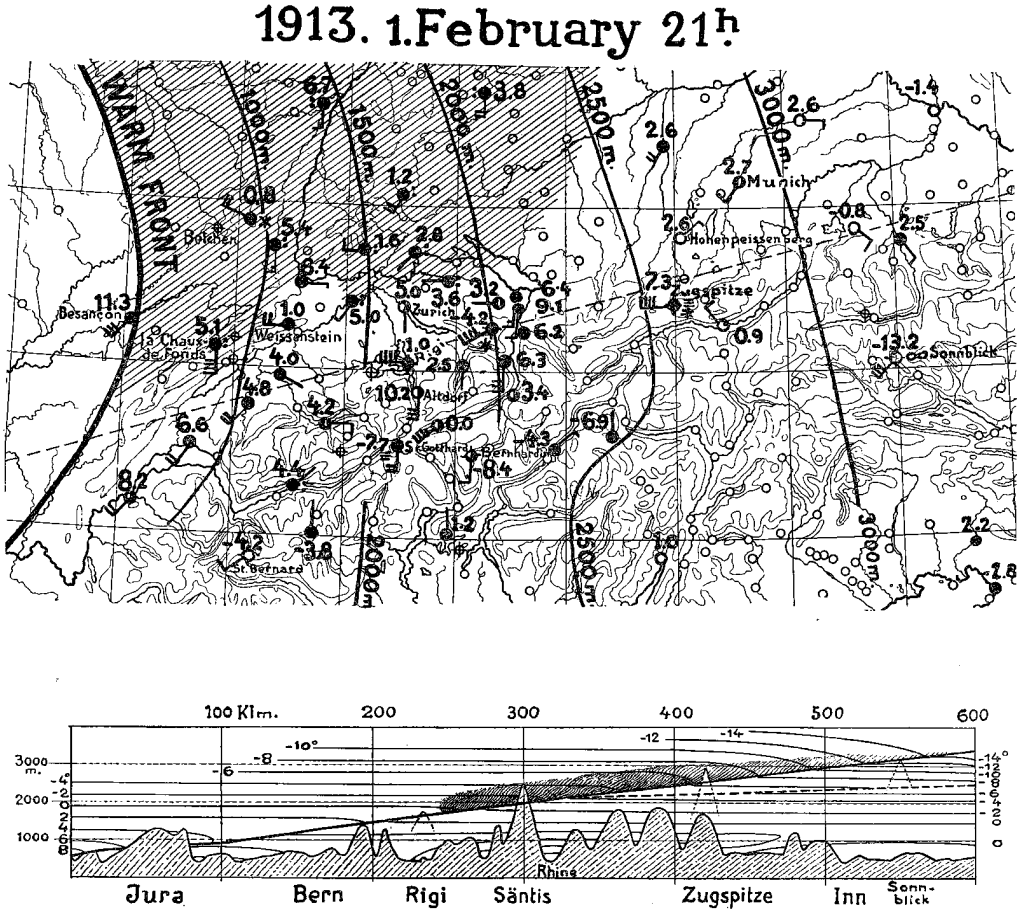

Fig. 3. Topography of the warm front surface.

warm sector current had started flowing through the French-Italian Alp passes, thus also making its push eastward on the south side of the Swiss—Austrian Alp chains.

In the cold air there was a south component of wind across the Alps strong enough to produce foehn on the northern slope. This is seen from the temperatures in the Reuss and Rhine valleys (Altdorf 456 m., 10°.2, Altstätten 449 m., 9°.1) which are several degrees higher than the temperatures at the same level on the plain. An interesting detail of this foehn situation appears in the Säntis region. Heiden (797 m.) and Wildhaus (1 115 m.) have got their air supply from the foehn current of the Rhine valley and show much higher temperatures than the neighbouring station St. Gallen (600 m.) on the western side of the Säntis massif. Arriving on the plain the foehn air mixes with the colder air or ascends above it, anyhow it is no longer visible in surface observations. Nevertheless, the foehn must have the effect of diminishing the content of moisture of the atmosphere into which it intrudes. This effect suffices to prevent precipitation on the

nearest part of the plain north of the Alps. In our case this dry zone extends nearly to the northern frontier of Switzerland. Farther north, over France and Germany, the warm front rain covers a broad zone indicated on the map by shading. From the dry zone one may observe the passage of the threatening warm front clouds overhead, and at the same time see the rain in the north, while the south horizon has a clear «Foehn segment» which persists over the slopes of the Alps.

The warm front phenomenon which we are going to examine is thus strongly influenced by the orography. This must always be remembered when the results are to be interpreted and applied to the free atmosphere.

Below the map on Fig. 3, there is a vertical section through the atmosphere along a straight line through Säntis with the azimuth S 75 W, approximately parallel to the warm sector current. Stations not far from this line are projected perpendicularly on the section. According to the registrations Säntis and Zugspitze were already some hours beforehand reached by the warm sector air, while Sonnblick was just at the point where the rise of temperature began. The warm front surface in the vertical section will thus pass below the tops of Säntis and Zugspitze and just touch the top of Sonnblick. On a somewhat lower level Rigi (1 787 m.) gives a good determination of the position of the warm front surface. The temperature is there + 1°.0 or exactly the same as on Weissenstein (1 285 m.) in the Jura farther west. The warm front surface must therefore pass below the top of Rigi and above Weissenstein. The inclination of the warm front surface is about $\frac{1}{200}$ in the upper part. Nearer to the ground it seems to be a little steeper.

On transferring these results to the map, we may draw a system of contour lines which give the topography of the warm front surface. Thereby the height of the surface derived from the observations of St. Bernard, St. Gotthard and Bernhardin appears too great to be fitted into the system of contour lines to the north of the Alps. This shows that the warm front surface must be at relatively higher level to the south than to the north of the Alps. This is not at all surprising when we take into consideration that all Swiss Alp passes (excepting that of Maloja in the Engadine) are higher than 2 000 metres and that the mean height of the chain is about 2 500 metres. Only where the cold air has a greater height than 2 500 metres (viz. in our case over Tyrol) it may communicate fairly unhindered from the south to the north side, so that differences of height may be levelled out.

It is interesting to note that the deformation of the contour lines of the warm front surface is similar to the well known deformation of the Alp isobars in front of approaching depressions (wedge of high pressure to the south and wedge of low pressure to the north). The statical effect of the cold wedge, therefore, acts on the pressure at the ground in a manner which accentuates the deformation of the Alp isobars. It is, however, not the only cause of the deformation of the pressure field, as also homogeneous south currents have similar effects.

The mountain observations also inform us about the position in space of the warm front clouds. Säntis had been in clouds since $17^1/_2{}^h$ and emerged at $21^1/_2{}^h$, the snowfall began at 16^h and ceased before the evening observation at 21^h. Zugspitze had fog from 19^h, and a slight snowfall had begun just before the evening observation. Sonnblick reports mist at the evening observation but cloudiness zero. The station has probably been in a veil of clouds which was still so transparent that it did not hide the stars. The relative humidity was 99 % and reached just afterwards 100 %.

According to Stüve the surfaces of subsidence are always less steep than the following warm front surface. Therefore, if we were to identify one of the surfaces of sub-

sidence on the Säntis thermogram with that on the Zugspitze (at 12^h) it should be that one passing at $16^3/_4{}^h$. Basing on this assumption, I have introduced a surface of subsidence on the vertical section. The surface has an inclination of about $\frac{1}{1000}$ and it joins with the steeper warm front surface at a level of about 2 000 metres. This is also in accordance with the fact that no surface of subsidence is to be seen in the registrations of Belchen.

When this very slightly inclined surface of subsidence gives such sudden rises of temperature as we observe them on the registrations of Säntis and Zugspitze, it must be

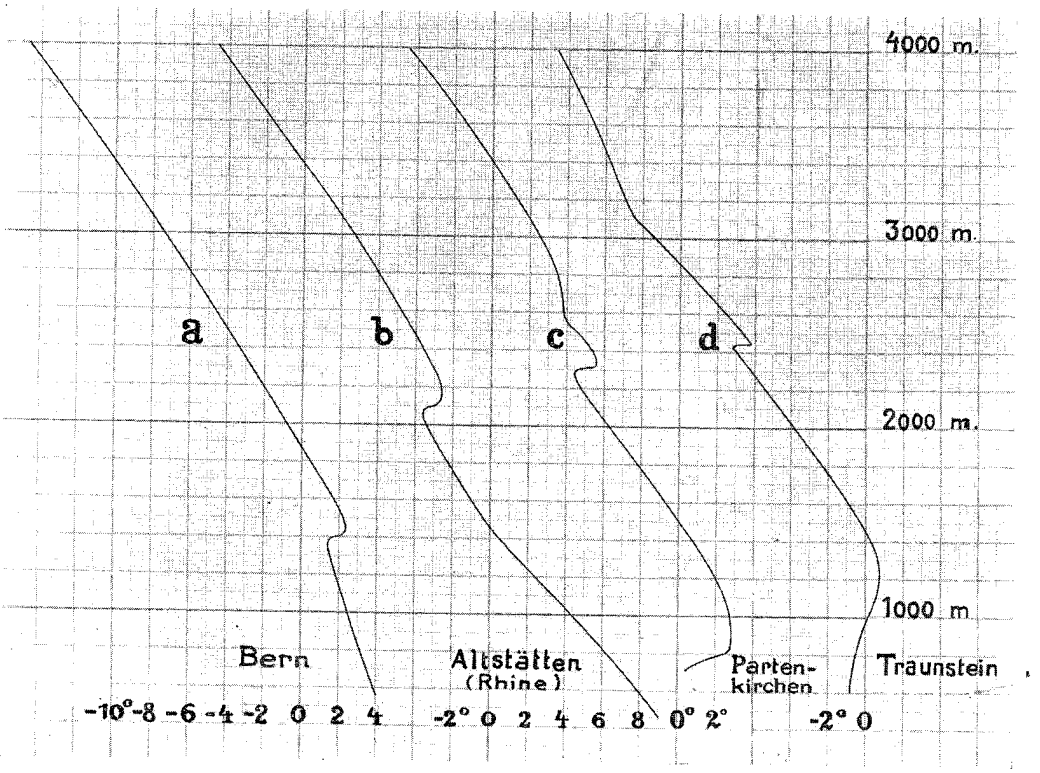

Fig. 4. Types of temperature-height curves at different distances from the warm front.

accompanied by a strong inversion of temperature (to be seen on the isotherm of $-6°$ on figure 3).

The isotherms on the vertical section have as much as possible been drawn in such a manner that a translation of the field would at fixed points give the change of temperature which is known from the thermograms. From the obtained system of isotherms we may again find the temperature-height curves which would have been registered during aerological ascents (ballon-sonde, kite or aeroplane). Fig. 4 gives some of these curves obtained at different places under the warm front surface. In Bern a well defined inversion would have been found. In the Rhine valley, the foehn current would in the lowest layers have given an almost adiabatic lapse rate, while aloft one would find a zone with normal lapse rate, and above this zone the warm front surface would appear as a small inversion of temperature. An ascent at Partenkirchen would have shown a shallow cold surface layer, then a layer of foehn, then the surface of subsidence as a distinct inversion of temperature, and finally at the top, the warm front surface represented by a layer about 400 metres thick merely characterized by a smaller lapse rate than the normal.

Still farther east one would get a similar type (d) only with the two surfaces at greater mutual distances and with the warm front surface still more degenerate.

In plains far from mountains, one would get the same sort of curves, only with elimination of the foehn phase.

This result has already been found by Stüve and Diesing. When I seize the opportunity of emphasizing their result once more, I do it in order to advise against the useless schematic search for real temperature *inversions* at the polar front surface. I feel it so much the more my duty to do this as I am unfortunately responsible for the false idea that the warm front and cold front surfaces should necessarily show true inversions of temperature associated with high relative humidity above and low underneath. In fact, this ideal case is not very common.*) For theoretical reasons one should expect to find it close to a well marked warm front, in our case represented by Bern or Altstätten. While the c and d types (sometimes with additional surfaces of subsidence) are much more likely to occur at greater distances from the front as well as in the cases of dege- neration. It is true that inversions of temperature are found as soon as one or more surfaces of subsidence are well developed. These inversions have, however, the driest air above. The warm front surface itself, very often appears merely as a layer of subnormal lapse rate, (and of course an increase of relative humidity upwards). It must therefore often fail to attract attention when a summary statistical analysis is made.

c. The Field of Motion in the Vicinity of the Warm Front Surface.

The Säntis registrations can be transferred to a representation in space of the registered elements. From the synoptic maps we have derived the result that the warm front moved with a velocity of about 60 km/h measured along the direction from S 75 W. 1 hour of the registration will consequently correspond to 60 km. horizontal distance. In order to retain the same orientation as in the vertical section of Fig. 3, we must reverse the sign of the abscissae, so that the new representation of the elements will get the aspect of a registration running from right to left.

For later analysis of the field of motion it has proved practical to use specific momentum instead of velocity, and we have therefore in Fig. 5 begun with a representation of the density. This curve has approximately the shape of the corresponding temperature curve turned upside down. The variations of pressure, which are also allowed for, are too small to have any important influence on the shape of the curve.

Underneath the ϱ curve there is a representation of wind velocity and direction, derived from the Säntis anemogram. The passage of the warm front surface about 19^h is characterized by a rapid increase of wind from 6.4 m./sec. on the cold side to 18.0 m./sec. in the warm sector.

The time which elapsed between these two extreme values of wind velocity was about half an hour (from $18^h\ 48^m$ to $19^h\ 20^m$). In the horizontal distance that corresponds to 32 kilometers and vertically to $\frac{32\,000}{200} = 160$ m. What we have hitherto called the warm front surface is thus an in our case inclined transitional layer about 160 m. thick. In this layer we have an intensive sliding motion between the two differently moving air masses.

This layer of sliding motion is marked by two stippled lines on the registrations of Fig. 5. Returning for a moment to the ϱ curve, we find that the two stippled lines enclose

*) One of the most «ideal» cases of a sounding through a warm front system is to be found on the weather bulletin of the Institut Royal Météorologique de Belgique of the 2nd of July, 1924 (diagram on the bulletin of the following day).

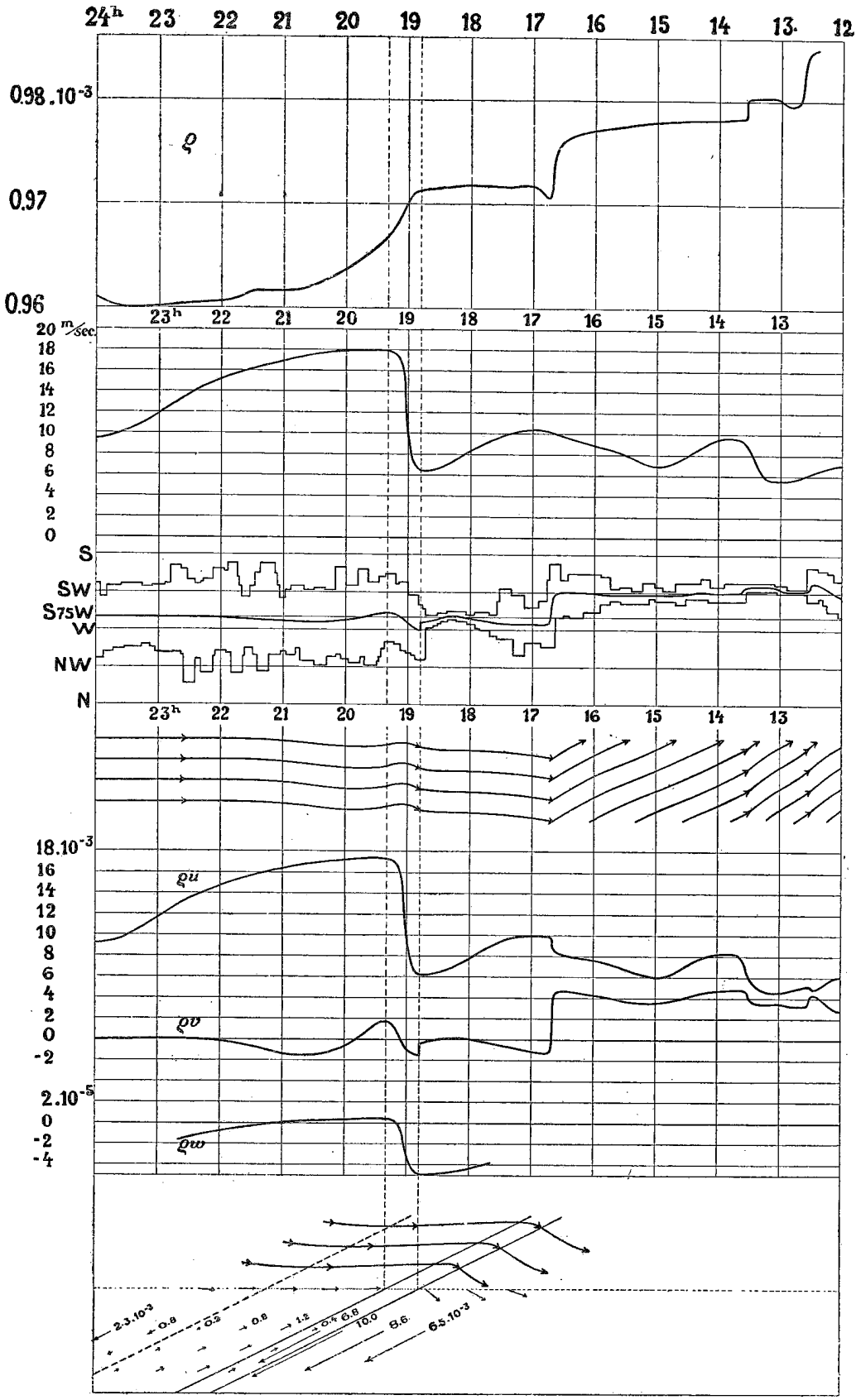

Fig. 5. Cross sections through the warm front system in 2 500 m. level.

part of the curve which has a great inclination. The layer of sliding is therefore at the same time a layer of transition from cold to warm air, and therefore probably contains a mixture of both. To the right of (or below) this mixed layer we may assume air of pure cold origin, to the left of (or above) pure warm sector air.

The registration of wind direction shows that there has been a strong turbulence especially during the periods of strongest wind. It has therefore been necessary to smooth out the particular oscillations of the wind vane and form a mean wind direction. This is represented by the curve beginning from the left at S 75 W and running along in the middle of the space covered by the registration of wind direction. The two stippled lines here enclose part of the registration where the wind is backing from W to S 70 W. At the transition to the cold air there is a sudden turn of wind but only to a small amount. The most characteristic feature of this part of the registration is the small turbulence in the cold air in comparison with that both in the transitional layer and in the warm sector. While there was a very small veer of wind at the passage of the warm front surface, a much greater veer of wind has already taken place during the passage of the nearest surface of subsidence (at $16^{3}/_{4}^{h}$). This is still better seen from the lines of flow which are constructed in a horizontal projection underneath the registration of wind direction. The discontinuity at the surface of subsidence is the most prominent feature of the lines of flow, while the warm front itself is not by far as distinct.

In order to find the vertical components we make the following assumptions concerning the field of motion in the vicinity of the warm front surface:

1. The contour lines of the warm front surface at the level of Säntis should have the azimuth N 15 W and thus be perpendicular to the azimuth S 75 W of the vertical section to which Figs. 3 and 5 refer.

2. The curvature of the surface should be negligible and its inclination $\frac{1}{200}$ measured in the direction S 75 W.

3. Specific momentum should have the same direction and intensity in all points of surfaces parallel to the warm front surface, and only vary from one of these surfaces to another.

These conditions can not be strictly derived from observations. But they are the simplest assumptions which can be made for arriving at a three dimensional picture of the field from the knowledge of the registrations. Condition 3 will of course only be valid in the nearest vicinity of the warm front surface, so that we must limit the construction of vertical motion to this region.

The above assumptions being made, we may draw conclusions concerning the vertical component of the motion.

The warm front surface moves with the velocity of 60 km./h. or 16.7 m./sec. measured along the direction from S 75° W. In the cold air just in front of the surface Säntis's wind has, however, only a component of 6.4 m./sec. in the same direction. As this air can not disappear it must have a descending component which would correspond to an apparent horizontal propagation of the surface of $16.7 - 6.4 = 10{,}3$ m./sec. Calculating with the inclination $\frac{1}{200}$ we get $\frac{10.3}{200} = 0.0515$ m./sec. as the value of the downward velocity component of the cold air just below the warm front surface.

In order to find the distribution of the vertical component within both of the air masses, we decompose the wind into a component u directed from S 75 W and another component v perpendicularly to this, viz. from S 15 E. We then multiply each of the components by the density ϱ, thus getting the rectangular components of specific mo-

mentum ϱu and ϱv which are represented in Fig. 5. To this field of specific momentum we may apply the equation of continuity, (see for instance V. Bjerknes: Dynamic Meteorology, II, Kinematics, p. 142)

$$\frac{\partial(\varrho w)}{\partial z} = -\left(\frac{\partial(\varrho u)}{\partial x} + \frac{\partial(\varrho v)}{\partial y}\right)$$

which gives the increase of vertical specific momentum, per unit vertical distance.

As the Y axis is parallel to the warm front surface, the derivative $\frac{\partial(\varrho v)}{\partial y}$ drops out according to condition 3, and the equation reduces itself to:

$$\frac{\partial(\varrho w)}{\partial z} = -\frac{\partial(\varrho u)}{\partial x}$$

The vertical component of specific momentum at the height h is thus found by an integration along z:

$$(\varrho w)_h = (\varrho w)_0 - \int_0^h \frac{\partial(\varrho u)}{\partial x}\, dz$$

If we choose the height 0 at the point where the path of integration passes from the cold air into the layer of transition, $(\varrho w)_0$ is known, and it only remains to determine the integral.

According to condition 3 the equiscalar surfaces of ϱu and likewise of $\frac{\partial(\varrho u)}{\partial x}$ run parallel to the warm front surface. Therefore, when starting from a point on the warm front surface, after a certain distance h along the Z axis, we arrive at the same equiscalar surface as we should have reached at the distance 200 h in the direction of the negative X axis. $\frac{\partial(\varrho u)}{\partial x}$ is thus the same function of z as of $-x$ provided that we make the units of the argument 200 times smaller. We may therefore in the above equation replace the argument z by x and get the following expression for $\partial(\varrho w)$ as a function of x:

$$\varrho w = (\varrho w)_0 + \frac{1}{200}\int_0^x \frac{\partial(\varrho u)}{\partial x}\, dx = (\varrho w)_0 + \frac{\varrho u - (\varrho u)_0}{200}$$

$$= \varrho_0\left(w_0 - \frac{u_0}{200}\right) + \frac{\varrho u}{200}$$

ϱ_0, the density of the cold air close to the boundary surface, is in our case equal to 0.0009713. w_0 and u_0 are respectively -0.0515 and 6.4, so that we get:

$$\varrho w = 0.0009713\left(-0.0515 - \frac{6\cdot 4}{200}\right) + \frac{\varrho u}{200}$$

$$= \frac{1}{200}(\varrho u - 0.0162)$$

From this equation we see that ϱw becomes equal to zero at the points where $\varrho u = 0.0162$. ϱw will be positive, that is, the motion ascending where $\varrho u > 0.0162$; in the rest of the field the motion will be descending. ϱw as a function of x gives a curve of the same shape as that of ϱu. In Fig. 5 it is introduced in a scale 100 times greater than that of the

horizontal components. As ϱ is very near $\frac{1}{1000}$, the three curves for ϱu, ϱv, and ϱw also give the approximate curves for u, v, and w, the two horizontal ones u and v in metres per second and the vertical w in centimeters pr. second.

From the representation by the rectangular components we may pass to the lines of flow in space by simple graphical integration. The resulting streamlines in a vertical projection (u and w components) are given in Fig. 5, in which the vertical scale is made 100 times greater than the horizontal. With this exaggeration of the vertical dimensions the downward motion in the cold air comes out quite distinctly, but in the warm current the inclination of the lines of flow is still very small. If referred to a system of co-ordinates which follows the motion of the surface, the lines of flow become straight lines exactly parallel to the warm front surface. This motion is reproduced below by a system of arrows the lengths of which are proportional to the magnitude of the vector. We see that cold air slides rapidly downwards and backwards relatively to the moving system. The warm air slides upwards and forwards in a zone which extends from the layer of transition about 120 kilometers into the warm sector. If we imagine this zone to be inclined parallel to the warm front surface it would correspond to a sheet with the thickness of 6—700 metres. This space is in fact filled with clouds (see Fig. 3). The absolute amount of the ascending component is very small, nowhere greater than 0.58 cm./sec., whereas the descending motion just beyond the warm front surface reaches the far greater value of 5.15 cm./sec. This preponderance of descending motion is certainly due to the foehn which blows below within the wedge of cold air. In our case the foehn proves to be almost strong enough to compensate the ascending component of the warm sector air which is climbing on the cold wedge. Nearer to the chain of the Alps the influence of the foehn is even strong enough to overcompensate every ascending motion at the warm front surface, thus making the warm front clouds dissolve. At an earlier stage when the warm front had not yet reached the Alp region, one would probably have found a similar shape of the w curve, only with the addition of an upwards vector of say 2 or 3 cm./sec. over the whole field. The limit between ascending and descending masses would then still remain within the layer of transition, but the ascending current would fill a greater space above the surface, with the effect that the clouds would be thicker and the precipitation stronger than in our case.

In order to find the distribution of vertical motion in the vicinity of the surface of subsidence we might have tried to use the analogous method. In that case, however, the result becomes very uncertain as it depends too much on the assumption made concerning the orientation in space of the surface of subsidence.*) With the orientation of contour lines parallel to those of the warm front surface (azimuth N 15 W) we get the result that the air above the surface slides slowly upwards relatively to the air underneath. With the azimuth N 33 W the result would be an almost horizontal sliding, and if the azimuth be beyond N 33 W the construction would give the result that the air above would slide downwards relatively to the air underneath. Such an orientation of the surface of subsidence is quite probable. It would mean that the warm front surface and the surface of subsidence in their southern parts diverge from each other, or in other words that the subsiding process has developed further in the southernmost end of the tongue of polar air than farther north in the polar atmosphere itself.

*) A small turn in the assumed orientation of the warm front surface has not by far the same effect on the construction of the vertical component of motion, as the uncertainty enters only at places where there also is a decided turn of wind direction.

IV. The Influence of the Vertical Motion on the Distribution of Temperature in the Vicinity of the Warm Front Surface.

The individual air masses which pass the top of the Säntis originate from different levels of the atmosphere, and provided that they have not been supplied with or lost heat, they arrive with the potential temperature of the level from where they started their vertical motion. We may thus use the temperatures to get an idea of the vertical displacements which have taken place. We shall thereby maintain from the foregoing chapter the

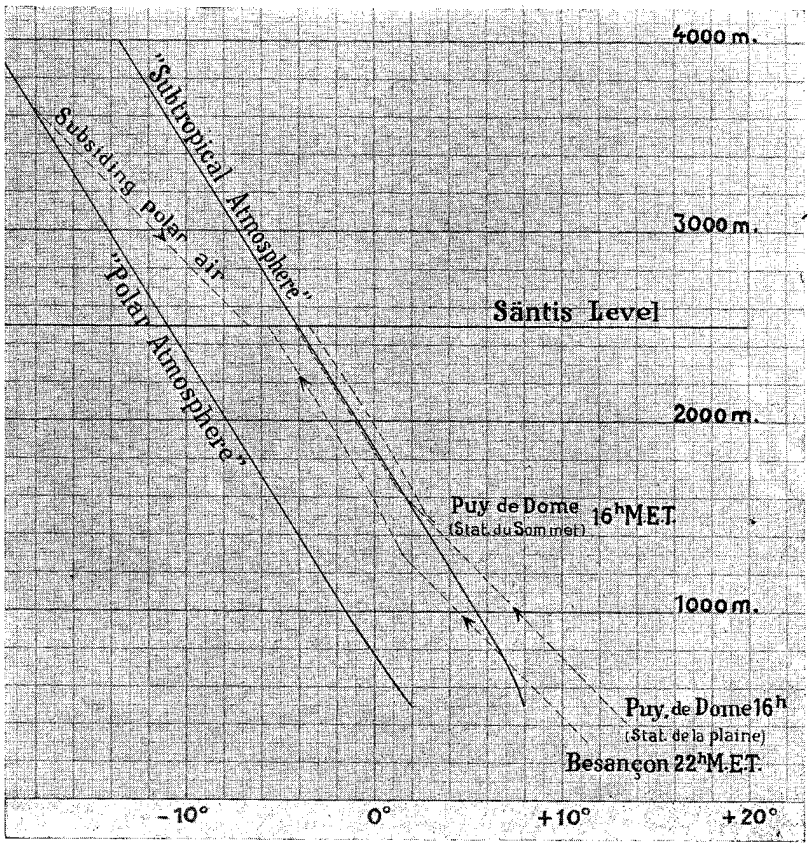

Fig. 6.

assumption that all air particles passing before $18^h\ 48^m$ originate from a polar atmosphere, and the air arriving after $19^h\ 20^m$ from a subtropical atmosphere. The air passing between these two epochs should then be a mixture from both «atmospheres». As representatives of these two «atmospheres» we may take the polar air as it was when arriving freshly from northern regions in the rear of the preceding depression, and the subtropical air as it was in the warmest part of the warm sector.

Fig. 6 contains the temperature-height curve of these two atmospheres based on the temperatures of surface and mountain stations, and extrapolated up to 4000 m. In the coldest part of the polar atmosphere Säntis had a temperature of — 11°.0. During the approach of the new depression the temperature rose, and just before arrival of the warm front surface it reached — 6°.6. If we assume that this heating has been produced

by dry adiabatic processes, the air mass in question must have originated from the level 3 650 m. in the «polar atmosphere», or 1 150 m. higher than Säntis. All the air between the warm front surface and the nearest surface of subsidence seems to originate from approximately the same height, whereas the air just underneath the latter surface has only sunk down from the level of 3 300 m., and so on.

The calculated vertical displacement would have been considerably greater if there were clouds in the layers in question at the beginning of the descending motion. In fact if we start with the values of temperature and humidity on Säntis at the noon observation and follow the process backwards, we find that the air mass would have been saturated from the level 2 900 m. and upwards. This indicates that the subsiding process in the cold air must really have had visible effects in the way of the wellknown dissolution of lower clouds (Cu, CuNb) under an arriving system of high clouds (CiSt, ASt).

As disturbing factors in the adiabatic processes we have especially to reckon with the effect of the warm front precipitation which falls down through the descending air masses of the cold wedge. This precipitation will usually be colder than the air through which it falls and therefore extract heat from the air. When the same air mass during a long period of time is exposed to this cooling effect the temperature will sink perceptibly. The same air will also receive the humidity which evaporates from the precipitation, and will thus get a higher relative humidity than one could expect after its downwards displacement. The above calculations of the height from which the subsiding air masses originate will consequently have a merely approximate validity.

Within the transitional layer the temperature rose from — 6°.6 to — 5°.3, but it was not until three hours later that the maximum temperature (— 4°.0) of the warm sector was reached. Thus, the foremost part of the warm sector contains air with temperatures from — 4°.0 to — 5°.3. It may seem plausible to explain these relatively cold temperatures in the foremost part of the warm sector by the adiabatic cooling in the ascending current, and we may try to test this assumption. It is thereby of course impossible to follow the adiabatic process backwards as the ascending air is saturated so that we cannot tell from Säntis's observations alone at which level the transition from dry to moist adiabatic occurred. We will therefore begin from the opposite end and try if an air particle leaving the ground in the warm sector would arrive at Säntis's level with the temperatures which was really observed in the ascending current. For this purpose we must choose stations that lie approximately to the W 15 S of Säntis as that has been the direction of the warm sector wind.

On Puy de Dôme (station de la plaine 399 m.) the warm front passed at about 13^h and the highest temperature of the warm sector (13°.7) was read at 16^h. At the same time the relative humidity was 50 %. If we were to let this air ascend, it would become saturated at 1 650 m. with a temperature of 1°.2. Upon further ascension the air changes its temperature in accordance with the moist adiabatic law and arrives at Säntis's level with — 4°.0. When we introduce these values into the graph of Fig. 6, we find that the moist adiabatic part of the curve almost coincides with the temperature-height curve which we have found for the warm sector over Switzerland. On carrying through the same calculations for the air mass which at 16^h was in level with Puy de Dôme (station du sommet 1 467 m.), we get similar results. It starts with a temperature 3°.2 and relative humidity 98 %, starts condensing at 1 550 m. with 2°.4, and reaches the level 2 500 m. with a temperature of — 3°.5. In Bordeaux (74 m.) further towards WSW the temperature at 15^h was 16°.9 and relative humidity 47 %, level of saturation 1 440 m. with 3°.2, and temperature at 2 500 m. level — 3°.2. We see from these examples that we cannot explain the foremost relatively cold part of the warm sector by the adiabatic cooling of the ascending air. Thanks to the small lapse rate during the

moist adiabatic phase the ascending air particles arrive at the level of 2500 m. with a temperature as high as, or even higher than, the maximum temperature observed on Säntis in the warm sector.

In order to give a temperature below — 4°.0 at Säntis's level the air must in some way lose heat during the ascension.

The amount of heat which is given off to the precipitation may in this case also be the deciding factor. As the cloud sheet has a thickness of 6—700 m., the precipitation, originating from the upper part of it, will be some degrees colder than the air further down in the same cloud. Also in this case we have to remember that the individual air masses climbing the warm front surface are influenced by precipitation during such a length of time that even a slow cooling may have appreciable effect.

The temperature of the foremost part of the warm sector would certainly also be diminished if this air were mixed up with particles from the underlying cold air. Such mixing would necessarily also have involved a transport of specific momentum from the one mass to the other with the effect of smoothening the rapid transition of wind velocity. By the analysis of the field of motion we have, however, found that the transition from the minimum wind velocity in the cold wedge up to the maximum velocity in the warm sector takes place in a layer not more than 160 metres thick. It therefore seems justified to conclude, as we have already done on page 13, that the zone of mixing is only as thick as about 160 metres. If this be true the direct mixing with the cold air should not be responsible for any loss of heat from the warm sector itself.

This conclusion is only valid for free air conditions. Close to the ground there is more possibility of mixing of the two air masses. In these layers the friction against the ground may reduce the velocity of the air so much that it cannot keep up to the motion of the whole system. In the case of a warm front, this would have the effect that a shallow cold air mass drags behind while the upper part of the warm front surface passes forwards with the velocity of the free air motion. In hilly country this shallow cold air will fill the protected valleys, where it can only very slowly mix with the warm current above. Stations in the valleys may therefore long after the passage of a warm front lie in a mixture of cold air and real warm sector air. We see this phenomenon, for instance, on Besançon (311 m.) and Lyon (299 m.). Both these stations have a slow continuous rise of temperature at the passage of the warm front, and their maximum temperatures in the warm sector, 11°.4 and 11°.1 respectively, are low in comparison with 14°.0 at Puy de Dôme (399 m.). In the case of air ascending from Besançon (introduced on Fig. 6) we get — 5°.6 for the 2500 m. level. This is practically the same temperature as we found in the foremost part of the warm sector close to the transitional layer.

Summing up, we may state that the cooling of the foremost part of the warm sector is in our case probably not due to direct mixing with the cold air, but more likely due to mixing which has taken place at the ground before the start of the ascending motion. In addition to this the cooling by contact with precipitation which is falling from higher layers is to be mentioned as an important factor.

Just after Säntis had emerged from the clouds there was again a slight rise of temperature. The simultaneous decrease of wind velocity indicated that a descending motion prevailed (see Fig. 5) and it was therefore natural to attribute the rise of temperature to the adiabatic heating of the descending air. The following fall of temperature after midnight coincides with an increase of wind, or in other words with the termination of the descending phase.

We may illustrate the results of our analysis of the Säntis thermogram in the scheme of Fig. 7. The polar atmosphere and the tropical atmosphere passing Säntis with perfectly abrupt changes in the meteorological elements at their mutual boundary would

have given the thermogram consisting of straight lines at right angles to each other. The shaded areas, which lie between this ideal temperature curve and the real thermogram, show the result of the modifying thermal processes in the polar and tropical atmospheres. The area to the left of the warm front represents the adiabatic heating in the subsiding polar air (and perhaps a little influence of the foehn). The small corner in the foremost part of the warm sector represents a cooling which is partly caused by the mixing, partly by precipitation. The small corner of the thermogram which overtops the ideal temperature curve is probably due to a phase of descending motion (perhaps of quite accidental character).

It still remains to consider the shape of the thermogram in the region of the cold front. I have, however, for the following reasons, abstained from a detailed analysis: The cold front brought great snowfall which made the thermograph register quite unsatis-

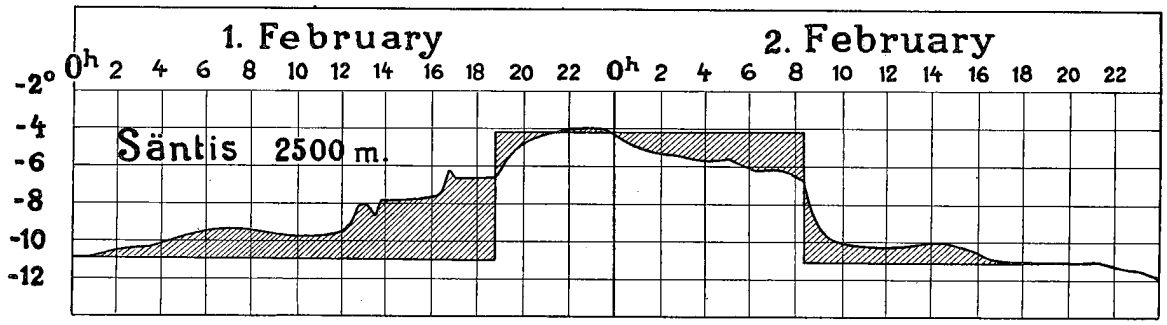

Fig. 7.

factorily. (The curve to the right of the cold front was chiefly reconstructed by aid of the readings at $7^h.30$, $10^h.30$, and $13^h.30$). Moreover, as the wind vane was oscillating in a violent and irregular manner and even making perfect revolutions in the gusts, the part of the wind registrations after the passage of the cold front was almost unusable. This is a wellknown peculiarity of Säntis in NW situations, and is probably due to the fact that the air currents tend to flow parallel to the chain of the Alps, and first at higher levels may flow across the direction of the chain. The Säntis seems to be a little too low for reaching the upper crosscurrent, but lies in a zone of conflict between the WSW current parallel to the Alps and the NW current above. As the WSW current is in this case only a deflected branch of the general NW current both convey air of the same cold origin.

As to the topography of the cold front surface we may only state that it was much steeper than the warm front surface $\left(\text{about } \frac{1}{30}\right)$. The fall of temperature was rather abrupt and coincided with the veer of wind. The slight fall of temperature which had already started 8 hours before the arrival of the cold front may be due to a slow continuous uplift of the warm sector air as a whole.

V. Dynamics of the Warm Front Surface.

We have seen from the foregoing diagnosis that the warm front surface is not a true surface of discontinuity, but a transitional layer with a rapid continuous change of the meteorological elements. Before passing to the dynamical prognosis we shall deduce equations characterizing the motion in the vicinity of such a «surface of approximate discontinuity». We thereby start from the equation for a true atmospheric surface of discontinuity given by V. Bjerknes*).

Let us suppose that we have a discontinuous change of density from ϱ to ϱ', of velocity from u, v, w to u', v', w', and of individual acceleration from $\dot{u}$, $\dot{v}$, $\dot{w}$ to $\dot{u}'$, $\dot{v}'$, $\dot{w}'$. Then the equation:

$$(1) \qquad [2(v^* \Omega_z - w^* \Omega_y) - \dot{u}^*]\, dx + [2(w^* \Omega_x - u^* \Omega_z) - \dot{v}^*]\, dy + \\ + [-g + (u^* \Omega_y - v^* \Omega_x) - \dot{w}^*]\, dz = 0$$

is valid for the air masses in the vicinity of the surface of discontinuity. In this equation g denotes the acceleration of gravity, Ω_x, Ω_y, and Ω_z denote the components of the angular velocity of earth's rotation; and u^*, v^*, w^*, $\dot{u}^*$, $\dot{v}^*$, $\dot{w}^*$ are abbreviations for the following expressions:

$$(2) \qquad u^* = \frac{\varrho u - \varrho' u'}{\varrho - \varrho'}; \quad v^* = \frac{\varrho v - \varrho' v'}{\varrho - \varrho'}; \quad w^* = \frac{\varrho w - \varrho' w'}{\varrho - \varrho'}$$

$$(3) \qquad \dot{u}^* = \frac{\varrho \dot{u} - \varrho' \dot{u}'}{\varrho - \varrho'}; \quad \dot{v}^* = \frac{\varrho \dot{v} - \varrho' \dot{v}'}{\varrho - \varrho'}; \quad \dot{w}^* = \frac{\varrho \dot{w} - \varrho' \dot{w}'}{\varrho - \varrho'}$$

The inclination with the horizontal of such a surface of discontinuity is given by:

$$(4) \qquad \frac{dz}{dx} = \frac{-2(v^* \Omega_z - w^* \Omega_y) + \dot{u}^*}{-g + 2(u^* \Omega_y - v^* \Omega_x) - \dot{w}^*}$$

$$(5) \qquad \frac{dz}{dy} = \frac{-2(w^* \Omega_x - u^* \Omega_z) + \dot{v}^*}{-g + 2(u^* \Omega_y - v^* \Omega_x) - \dot{w}^*}$$

Let us take an element of the surface of discontinuity where the inclination is known:

$$(6) \qquad \frac{dz}{dx} = \operatorname{tg} \Theta_x; \qquad \frac{dz}{dy} = \operatorname{tg} \Theta_y$$

Likewise we will consider the densities ϱ and ϱ', and the velocities u, v, w and u', v', w' as known quantities.

In the equations (4) and (5) the three quantities $\dot{u}^*$, $\dot{v}^*$, and $\dot{w}^*$ still remain unknown, but we only need to stipulate another relation between these three quantities in order to be able to determine all of them. For this reason we shall assume that the element of the surface retains an unaltered inclination and moves with constant velocity and that the curvature of the surface in the region of this element may be neglected. Then the

*) V. Bjerknes: «On the Dynamics of the Circular Vortex with Applications to the Atmosphere and Atmospheric Vortex and Wave Motions». Geofysiske Publikationer Vol. II, No. 4, p. 49.

acceleration vector will on both sides of the surface be directed tangentially to the surface element:

$$\dot{w} = \dot{u} \operatorname{tg} \Theta_x + \dot{v} \operatorname{tg} \Theta_y ; \qquad \dot{w}' = \dot{u}' \operatorname{tg} \Theta_x + \dot{v}' \operatorname{tg} \Theta_y \tag{7}$$

This also involves:

$$\dot{w}^* = \frac{\varrho (\dot{u} \operatorname{tg} \Theta_x + \dot{v} \operatorname{tg} \Theta_y) - \varrho' (\dot{u}' \operatorname{tg} \Theta_x + \dot{v}' \operatorname{tg} \Theta_y)}{\varrho - \varrho'} = \dot{u}^* \operatorname{tg} \Theta_x + \dot{v}^* \operatorname{tg} \Theta_y \tag{8}$$

which is the desired relation between $\dot{u}^*$, $\dot{v}^*$, and $\dot{w}^*$.

We may now by aid of equation (8) eliminate $\dot{w}^*$ from the equation (4) and (5) and then solve these equations with respect to $\dot{u}^*$ and $\dot{v}^*$. We then get the rather long expressions:

$$\dot{u}^* = \frac{(1 + \operatorname{tg}^2 \Theta_y) [2 (v^* \Omega_z - w^* \Omega_y) - \operatorname{tg} \Theta_x (g - 2 (u^* \Omega_y - v^* \Omega_x))] \ldots}{\ldots - \operatorname{tg} \Theta_x \operatorname{tg} \Theta_y [2 (w^* \Omega_x - v^* \Omega_z) - \operatorname{tg} \Theta_y (g - 2 (u^* \Omega_y - v^* \Omega_x))]} \tag{9}$$
$$(1 + \operatorname{tg}^2 \Theta_x) (1 + \operatorname{tg}^2 \Theta_y) - \operatorname{tg}^2 \Theta_x \operatorname{tg}^2 \Theta_y$$

$$\dot{v}^* = \frac{(1 + \operatorname{tg}^2 \Theta_x) [2 (w^* \Omega_x - u^* \Omega_z) - \operatorname{tg} \Theta_y (g - 2 (u^* \Omega_y - w^* \Omega_x))] \ldots}{\ldots - \operatorname{tg} \Theta_x \operatorname{tg} \Theta_y [2 (v^* \Omega_z - w^* \Omega_y) - \operatorname{tg} \Theta_x (g - 2 (u^* \Omega_y - v^* \Omega_x))]} \tag{10}$$
$$(1 + \operatorname{tg}^2 \Theta_x) (1 + \operatorname{tg}^2 \Theta_y) - \operatorname{tg}^2 \Theta_x \operatorname{tg}^2 \Theta_y$$

When we take into consideration that tg Θ_x and tg Θ_y are of the order of magnitude $\frac{1}{100}$, we may, however, simplify the above expressions considerably. The denominator becomes practically equal to 1; and the second term of the numerator becomes negligible, as it will have an order of magnitude 10 000 times smaller than the first term, we may further neglect $\operatorname{tg}^2 \Theta_x$ and $\operatorname{tg}^2 \Theta_y$ in comparison with 1, and get:

$$\dot{u}^* = 2 (v^* \Omega_z - w^* \Omega_y) - \operatorname{tg} \Theta_x (g - 2 (u^* \Omega_y - v^* \Omega_x)) \tag{11}$$

$$\dot{v}^* = 2 (w^* \Omega_x - u^* \Omega_z) - \operatorname{tg} \Theta_y (g - 2 (u^* \Omega_y - v^* \Omega_x)) \tag{12}$$

When we further take into consideration that the vertical velocity component is usually about $\frac{1}{100}$ of the horizontal component, we may, when no great exactness is needed, neglect $w^* \Omega_y$ in comparison with $v^* \Omega_z$ and $w^* \Omega_x$ in comparison with $u^* \Omega_z$. Finally, we may with the same degree of approximation neglect $2 (u^* \Omega_y - v^* \Omega_x)$ in comparison with g.

The equations (11) and (12) then reduce themselves to the very simple form:

$$\dot{u}^* = 2 v^* \Omega_z - g \operatorname{tg} \Theta_x \tag{13}$$

$$\dot{v}^* = - 2 u^* \Omega_z - g \operatorname{tg} \Theta_y \tag{14}$$

Or still simpler when we turn the system of co-ordinates so that, for instance, Θ_y becomes equal to zero:

$$\dot{u}^* = 2 v^* \Omega_z - g \operatorname{tg} \Theta_x \tag{15}$$

$$\dot{v}^* = - 2 u^* \Omega_z \tag{16}$$

Thereby also the relation (8) is reduced to:

$$\dot{w}^* = \dot{u}^* \operatorname{tg} \Theta_x = (2 v^* \Omega_z - g \operatorname{tg} \Theta_x) \operatorname{tg} \Theta_x \tag{17}$$

We obtain the most practical form for discussion when we re-introduce the expressions (2) and (3) for u^*, v^*, w^*, $\dot{u}^*$, $\dot{v}^*$, $\dot{w}^*$, and multiply the equations by $(\varrho - \varrho')$

$$\varrho\dot{u} - \varrho'\dot{u}' = 2\Omega_z(\varrho v - \varrho' v') - g \operatorname{tg} \Theta_x (\varrho - \varrho') \tag{18}$$

$$\varrho\dot{v} - \varrho'\dot{v}' = -2\Omega_z(\varrho u - \varrho' u') \tag{19}$$

$$\varrho\dot{w} - \varrho'\dot{w}' = (\varrho\dot{u} - \varrho'\dot{u}') \operatorname{tg} \Theta_x \tag{20}$$

The left sides now contain the difference of the product of density and acceleration formed on both sides of the surface of discontinuity. This difference represents a measure of the acceleration of the two air masses relatively to each other. We may denote this quantity «acceleration of shearing momentum».

The x and z components which together represent the «shearing momentum» in direction of the maximum inclination of the surface, depend on one term due to gravity and one term due to the earth's rotation. The gravity term is proportional to the inclination $\operatorname{tg} \Theta_x$ of the surface and to the discontinuity of density $(\varrho - \varrho')$, and acts in such a manner that the lightest of the two air masses should slide upwards relatively to the heavier one. The term due to the earth's rotation depends on the difference of the y-components of momentum $(\varrho v - \varrho' v')$ directed along the contour lines of the surface. This term may according to circumstances either assist or counteract the gravity term.

The y component of the «acceleration of shearing momentum», which is directed along the contour lines, merely depends on a term due to the earth's rotation, the amount of which varies proportionally to the negative «shearing momentum» of the x components.

In the special case:

$$2\Omega_z(\varrho v - \varrho' v') - g \operatorname{tg} \Theta_x (\varrho - \varrho') = 0 \tag{21}$$

we get no «acceleration of shearing momentum» of the x and z components. A shear along the contour lines:

$$\varrho v - \varrho' v' = \frac{g \operatorname{tg} \Theta_x (\varrho - \varrho')}{2\Omega_z} \tag{22}$$

is thus sufficient to compensate the effect of the gravity term. According to equation (19), $\varrho v - \varrho' v'$ will only keep this constant value if the two other shears are zero, viz: $\varrho u - \varrho' u' = 0$, $\varrho w - \varrho' w' = 0$.

If we solve equation (22) with respect to $\operatorname{tg} \Theta_x$ we get:

$$\operatorname{tg} \Theta_x = \frac{2\Omega_z}{g} \cdot \frac{\varrho v - \varrho' v'}{\varrho - \varrho'} \tag{23}$$

which is identical with the classical formula of Margules for the inclination of surfaces of discontinuity between air masses moving horizontally and tangentially to their mutual boundary surface. Formula (23) is also valid for the same system moving horizontally without acceleration.

If we were allowed to put

$$\frac{du^*}{dt} = \dot{u}^*; \qquad \frac{dv^*}{dt} = \dot{v}^*; \qquad \frac{dw^*}{dt} = \dot{w}^* \tag{24}$$

and further to replace the operator $\frac{d}{dt}$, denoting differentiation following the motion of the medium, by the operator $\frac{\partial}{\partial t}$, denoting partial differentiation with respect to time, the equations (15, 16, 17) would have a simple integral.

The first of these conditions would be fulfilled if ϱ and ϱ' remained constant with time for each individual particle. The second condition implies that u^*, v^*, and w^* at every given moment should in all points of the boundary surface have the same values, thus merely being functions of time. Both conditions may be fulfilled with good approximation in the case of small motions.

The result of the integration is:

$$u^* = \left(v_0^* - \frac{g \operatorname{tg} \Theta_x}{2\Omega_z}\right) \sin 2\Omega_z t + u_0^* \cos 2\Omega_z t \tag{25}$$

$$v^* = \frac{g \operatorname{tg} \Theta_x}{2\Omega_z} + \left(v_0^* - \frac{g \operatorname{tg} \Theta_x}{2\Omega_z}\right) \cos 2\Omega_z t - u_0^* \sin 2\Omega_z t \tag{26}$$

$$w^* = u^* \operatorname{tg} \Theta_x \tag{27}$$

where u_0^*, v_0^*, and w_0^* mean the initial values of u^*, v^*, and w^* at the time $t = 0$. The components of shearing momentum thus become periodic functions of time with the period $\frac{\pi}{\Omega_z}$. The amplitudes depend on the initial shear at the time $t = 0$. There is only one initial state which gives the amplitudes zero, namely:

$$u_0^* = 0$$
$$v_0^* = \frac{g \operatorname{tg} \Theta_x}{2\Omega_z}$$

This state is identical with that of a pure horizontal shear to which the formula of Margules (23) refers. All other initial values give a shear of an oscillatory character around the steady state of motion represented by the pure horizontal shear.

The integration has not the generality required for a full discussion of the stability of a surface of discontinuity in case of disturbances of any character. We have only treated an «oscillating shear», which takes place without any deformation of the boundary surface. The result is, however, of interest in as much as it shows that the pure horizontal shear, dealt with in the formula of Margules (23), is a stable one, as regards a special case of disturbances, those which do not involve deformations of the discontinuity surface itself.

In the case of «approximate discontinuity», with which we have to deal, we may consider the warm front surface as consisting of parallel surfaces of strict discontinuity infinitely near to each other. We may then apply the shearing equations to each of them. For this purpose we write the equations in the form (18) and (19)

$$\varrho \dot{u} - \varrho' \dot{u}' = 2\Omega_z (\varrho v - \varrho' v') - g \operatorname{tg} \Theta_x (\varrho - \varrho')$$

$$\varrho \dot{v} - \varrho' \dot{v}' = -2\Omega_z (\varrho u - \varrho' u')$$

When u, $\dot{u}$, v, $\dot{v}$, and ϱ refer to points infinitely near those of u', $\dot{u}'$, v', $\dot{v}'$, and ϱ', we may replace the differences by differentials and get:

$$\frac{\partial(\varrho\dot{u})}{\partial x} = 2\Omega_z \frac{\partial(\varrho v)}{\partial x} - g \operatorname{tg} \Theta \frac{\partial \varrho}{\partial x} \tag{28}$$

$$\frac{\partial(\varrho\dot{v})}{\partial x} = -2\Omega_z \frac{\partial(\varrho u)}{\partial x} \tag{29}$$

The equations indicate how much the particles of one sliding surface accelerate relatively to the particles of the neighbouring surface. In order to find the acceleration relatively to the ground we must start from a point where the acceleration is known as say at $x = 0$ and perform the integration along x:

$$\begin{aligned} \varrho\dot{u} &= (\varrho\dot{u})_0 + \int_0^x \frac{\partial(\varrho\dot{u})}{\partial x} dx = (\varrho\dot{u})_0 + 2\Omega_z \int_0^x \frac{\partial(\varrho v)}{\partial x} dx - g \operatorname{tg} \Theta_x \int_0^x \frac{\partial \varrho}{\partial x} dx \\ &= (\varrho\dot{u})_0 + 2\Omega_z [\varrho v - (\varrho v)_0] - g \operatorname{tg} \Theta_x (\varrho - \varrho_0) \end{aligned} \tag{30}$$

$$\begin{aligned} \varrho\dot{v} &= (\varrho\dot{v})_0 + \int_0^x \frac{\partial(\varrho\dot{v})}{\partial x} dx = (\varrho\dot{v})_0 - 2\Omega_z \int_0^x \frac{\partial(\varrho u)}{\partial x} dx \\ &= (\varrho\dot{v})_0 - 2\Omega_z [\varrho u - (\varrho u)_0] \end{aligned} \tag{31}$$

The z component remains as before equal to the x component multiplied by $\operatorname{tg} \Theta_x$:

$$\varrho\dot{w} = \varrho\dot{u} \operatorname{tg} \Theta_x \tag{32}$$

In this form the equations may be applied also to those boundary surfaces at which the discontinuous change of the elements is replaced by a rapid continuous change in a transitional zone.

We must, however, in doing so remember that the equations are deduced under the assumption that the boundary surface should undergo no deformation and propagate with constant velocity. In other words, the elements should be independent of time when referred to a system of co-ordinates which follows the motion of the boundary surface. This condition is never strictly fulfilled, and deviations from it will have effects not contained in our results. The idealization made in the equations is, however, equivalent to the assumption made when transferring the registrations at a fixed point into a representation of the elements in space, also then we assumed a constant propagation with unaltered profile. Generally speaking, one may expect that the shearing motion, for which the equations are valid, will already give a good approximation to the real field of motion in the vicinity of atmospheric boundary surfaces. The rest of the motion, which is responsible for all deformation and change of velocity of the surface, is not less important for the whole development, but it is numerically smaller than the shearing component and needs ample time for giving deformations of any importance.

Prognostic Application of the Preceding Formulae.

We shall apply the equations (30), (31) to the air on both sides of the warm front surface in order to find the distribution of acceleration $\varrho\dot{u}$, $\varrho\dot{v}$, $\varrho\dot{w}$. The equations only give «relative accelerations» — the difference between the acceleration at whatever point

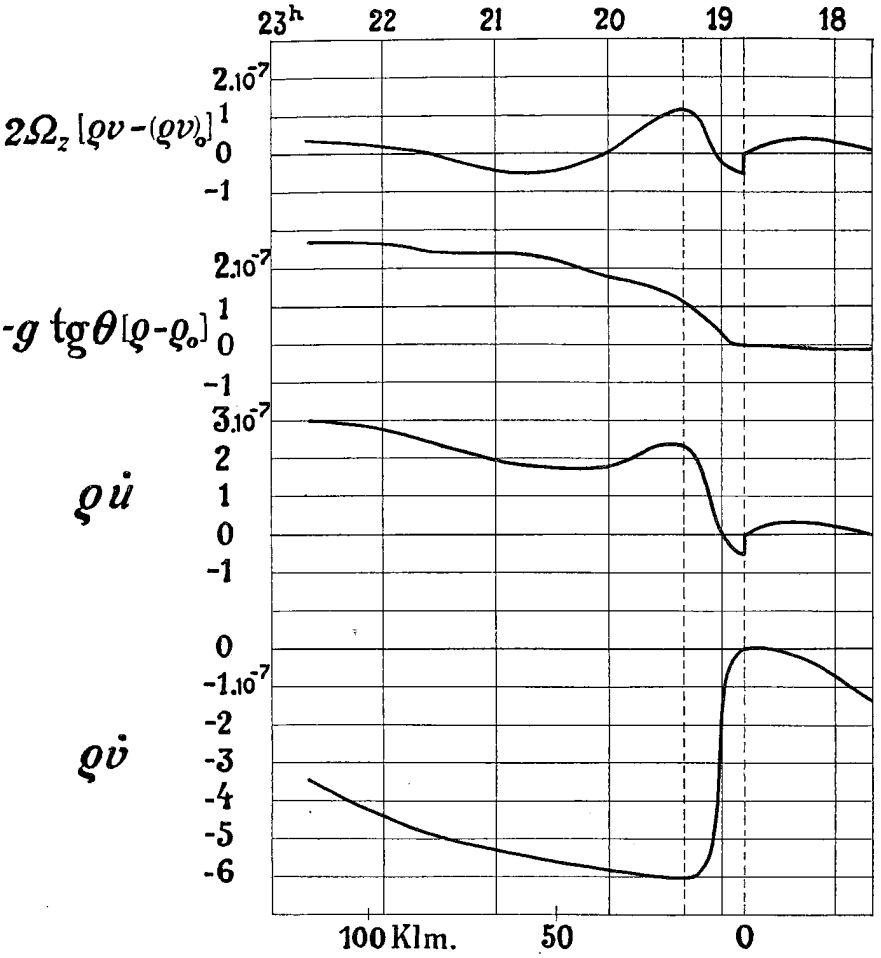

$$\varrho\dot{u} = 2\Omega_z[\varrho v - (\varrho v)_o] - g\ \mathrm{tg}\theta\,[\varrho - \varrho_o]$$
$$\varrho\dot{v} = -2\Omega_z[\varrho u - (\varrho u)_o]$$

Fig. 8. Graphical construction of the field of acceleration.

with «abscissa» x and the acceleration at the point $x = 0$. We may choose the point $x = 0$ just where the X axis passes from the cold wedge into the transitional layer. The acceleration which we calculate for the rest of the field is then the acceleration relative to the cold air particles just underneath the warm front surface. The acceleration relative to the earth could only be found by an integration performed from the ground up to 2 500 m. level, and would need observational data which we have not at our disposal. The acceleration relative to the ground would, however, be represented by curves of exactly

the same shape as those which we find for the acceleration relative to a certain particle, only with the addition of a constant vector $(\varrho\dot{u})_0$, $(\varrho\dot{v})_0$, $(\varrho\dot{w})_0$ over the whole field.

Fig. 8 gives a representation of the different terms which are contained in the equations (30), (31), as functions of x. The first term is a product of the constant factor $2\,\Omega_z$ (which in our case is $2\Omega \sin 47^\circ\,15' = 1{,}07.10^{-4}$) and the difference between ϱv and $(\varrho v)_0$. The resulting curve has the same shape as that of ϱv on Fig. 5. The only difference is an alteration of the scale and a displacement of the numerical values along the axis of ordinates.

The next term is a product of the constant factor, $-g\,\mathrm{tg}\,\Theta$ (in our case equal to $-4{,}9.10^{-2}$) and the difference between the densities ϱ and ϱ_0. The resulting curve has the same shape as the ϱ curve of Fig. 5, turned upside down.

$\varrho\dot{u}$ which is the sum of these two terms is represented by the next curve of Fig. 8.

$\varrho\dot{v}$ which merely depends on the term $-2\Omega_z\,[\varrho u - (\varrho u_0)]$ is represented by a curve which is obtained by turning the ϱu curve of Fig. 5 upside down and altering its scale.

The obtained functions representing $\varrho\dot{u}$ and $\varrho\dot{v}$ have the order of magnitude 10^{-7}. As ϱ is approximately 1.10^{-3} over the whole field, we may pass to $\dot{u}$ and $\dot{v}$ merely by an alteration of the unit of the scale from 10^{-7} to 10^{-4}.

The calculation shows in what manner the system of motion found by Säntis's registration would change under the influence of the field of forces which are implicitly given by the same registrations. In this way we arrive at a mathematical forecast of future motion which we may test on the maps.

We see from the $\dot{u}$ curve that the individual accelerations on the warm side of the surface are positive, when the acceleration of the nearest part of the cold mass is put equal to zero. In other words, the strong WSW wind in the warm sector should accelerate relatively to the more moderate WSW component in front. This would mean an increased sliding along the direction of maximum inclination on the warm front surface. We do not know, however, whether this increased sliding will appear as an increase of upward motion on the warm side or an increase of downward motion on the cold side. The latter possibility seems to be the most probable as the visible result of upward sliding — warm front precipitation — decreases during the continued eastward propagation. Simultaneously, the downward motion in the cold wedge seems to augment (more pronounced south foehn in Bavaria than in Switzerland).

The $\dot{v}$ curve shows us that the individual acceleration in the warm sector is negative when referred to the cold air in front as non accelerated. The negative $\dot{v}$ means that the air particles passing Säntis should curve to the right. In fact, it is probable that they do so, as the warm sector current which on the Säntis has the direction of about S 75 W will tend to keep parallel to the chain of the Alps, i. e., curve slightly towards the right. The acceleration due to the curvature of the path along the Alps can, however, hardly be estimated higher than $0{,}45.10^{-4}$ (curvature $0{,}25.10^{-5}$, and wind velocity 18 m./sec.), so that great part of the relative acceleration remains unexplained. We therefore arrive at the result that the cold air particles which pass Säntis just before the warm front must have an acceleration component of about 5.10^{-4} in (positive) northward direction.

The cold air particles just underneath the warm front surface have thus a negative $\dot{u}$ and $\dot{w}$, and a great positive $\dot{v}$. At the moment when the particles pass Säntis they produce a wind from WSW 6.4 m./sec. According to the calculated accelerations the same particles will later move with a decreasing west component and a rapidly increasing south component, and consequently give successive winds from SW, SSW, S, etc. In other words, the particles will blow along a cyclonically curved trajectory and pass north-

wards in front of the eastward moving depression. If the acceleration $\dot{v}$ retains a value of about 5.10^{-4}, the component v of the motion would increase 5 m./sec. in 3 hours and would reach gale force after 12 hours. We may thus for the morning of the 2nd of February, according to pure dynamical principles, forecast strong southerly winds over eastern Germany in front of the depression. The map (Fig. 1) shows that these strong south winds have really arisen, as may be seen from the steep pressure gradient between Breslau and the centre of the depression (Schneekoppe SW Beaufort 10). The strong pressure gradient in front of the depression was not to be observed over Western Europe the day before, and we have thus in fact derived from the Säntis registrations an important change of structure which was to take place in the depression.

I do not pretend that this forecast could not have been made by qualitative empirical methods (for instance, isallobaric methods). The chief point is that the mentioned forecast has been deduced directly from the hydrodynamical equations, and that it could have been given a quantitative form, provided that all observational data had been at hand.

VII. General Consequences.

The dynamical analysis of the warm front surface which we have carried through gives some results which may be generalized. When we consider an atmospheric boundary surface in the shape of a plane which retains constant inclination (contour lines parallel to the Y axis), the equations (28) and (29)

$$\frac{\partial(\varrho\dot{u})}{\partial x} = 2\Omega_z \frac{\partial(\varrho v)}{\partial x} - g \operatorname{tg} \Theta \frac{\partial \varrho}{\partial x}$$

$$\frac{\partial(\varrho\dot{v})}{\partial x} = -2\Omega_z \frac{\partial(\varrho u)}{\partial x}$$

are valid for the nearest vicinity of the surface. These equations also remain valid when the boundary surface is moving with constant velocity and the system of co-ordinates follows this motion. We shall choose the orientation of the system of co-ordinates in such a manner that Θ comes in the first quadrant, in other words, that an observer sees the cold wedge to the right when looking in the positive Y direction (Fig. 9 a).

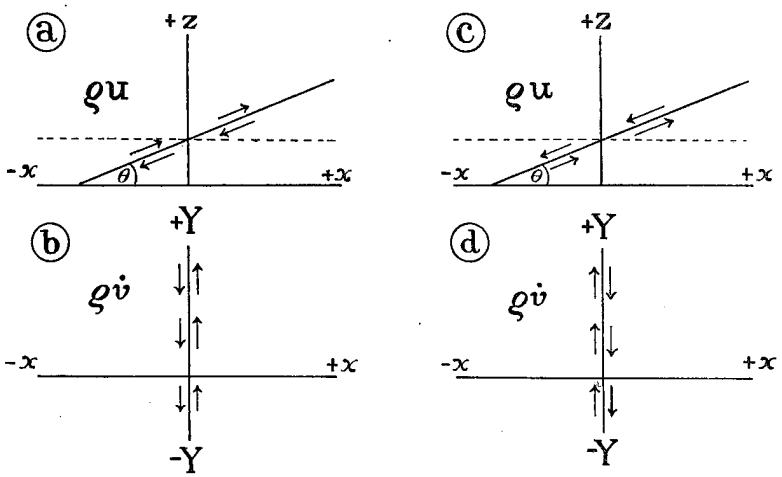

Fig. 9. Accelerations due to upward and downward sliding.

In all cases when the warm air has a component of sliding upwards on the cold wedge $\frac{\partial(\varrho u)}{\partial x}$ is negative in the vicinity of the boundary surface, so that $\frac{\partial(\varrho \dot{v})}{\partial x}$ becomes a positive quantity (according to equation (29), Ω_z being positive on the northern hemisphere). The motion represented by Fig. 9 a will thus correspond to a system of acceleration like that of figure 9 b.

In the same way we may deduce that a system of motion like that of figure 9 c, where the warm air slides downwards relatively to the cold, will correspond to a system of acceleration like that of figure 9 d.

All accelerations mentioned are individual ones. They are identical with the acceleration at a fixed point in the moving system of co-ordinates, provided that $\frac{\partial v}{\partial y} = 0$, i. e., that the component v has the same value all along the same contour line of the surface. Our discussion must therefore be confined to the case $\frac{\partial v}{\partial y} = 0$, but if sufficient data are at hand it is not difficult also to treat the more general case.

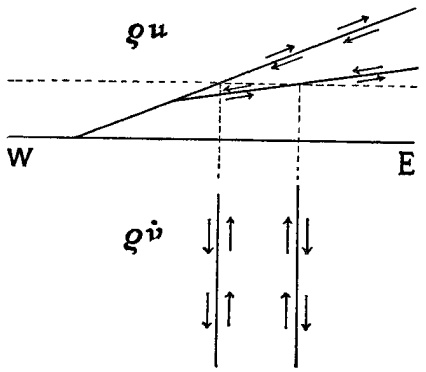

Fig. 10. Accelerations in a system of warm front surface and surface of subsidence.

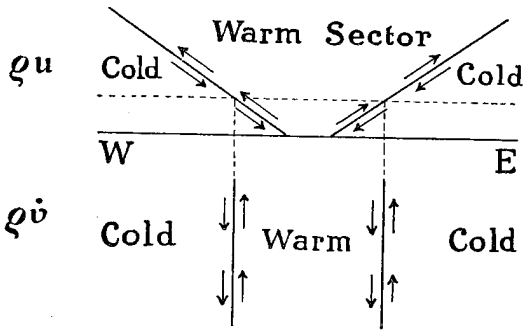

Fig. 11. Accelerations favourable for the formation of a V shaped depression.

The category of Fig. 9 a comprises all warm front surfaces and likewise the lowest parts of all cold front surfaces. (It is unusual to see a cold front surface advancing from the east, but we only need to imagine Fig. 9 a to be a section through a usual eastgoing cold front which is seen from the north.) The corresponding system of acceleration (Fig. 9 b) shows that there is a tendency to the formation of a discontinuity of the tangential components. This appears on the synoptic map as the formation of a line of wind discontinuity. Along these lines of wind discontinuity, there is a concentration of vorticity of positive (cyclonic) sign, which is constantly reinforced as long as the warm air has a sliding component upwards on the cold wedge.

All surfaces of subsidence belong to the category of Fig. 9 c. Likewise the upper part of many cold front surfaces at which the warm air moves faster forwards than the cold wedge underneath*). The distribution of acceleration (Fig. 9 d) is in this case such a one that it causes annihilation of cyclonic vorticity.

We may mention some practical consequences of equation (29):

In an ordinary system of a surface of subsidence and a warm front surface (Fig. 10) we get the result that *the air mass contained between the two surfaces has a northward acceleration both in relation to the air underneath and in relation to the air of the warm sector above.*

*) Compare Stüve: l. c. page 115.

In the situation of Fig. 11, the air in the narrow warm sector will have an acceleration southwards relatively to the cold air in front, and an acceleration northwards relatively to the cold air behind. The two cold wedges will consequently have a great mutual acceleration — the eastern northwards and the western southwards. In other words, there will be a strong tendency to the formation of a V shaped trough during the occlusion of the cyclone.

In other cases we may have a motion like that on Fig. 12 with a downward sliding of the warm air on the upper and greater part of the cold front surface. When we abstract from the lowest part, which has conditions identical with those of the foregoing example, we get the result that the warm air accelerates southwards relatively to both of the cold wedges. The two cold air masses which meet each other at the occlusion will consequently have accelerations which do not differ very much from each other, and there will be less tendency towards the formation of a V shaped trough.

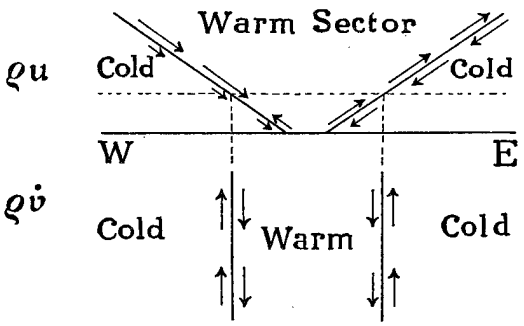

Fig. 12. Accelerations not favourable for the formation of a V shaped depression.

Equation (28) gives us another classification of the different atmospheric boundary surfaces. We may distinguish the following two cases from each other:

$$\frac{\partial(\varrho \dot{u})}{\partial x} < 0, \quad \text{i. e.:} \frac{\partial(\varrho v)}{\partial x} < \frac{g}{2\Omega_z} \operatorname{tg} \Theta \frac{\partial \varrho}{\partial x}$$

$$\frac{\partial(\varrho \dot{u})}{\partial x} > 0, \quad \text{i. e.:} \frac{\partial(\varrho v)}{\partial x} > \frac{g}{2\Omega_z} \operatorname{tg} \Theta \frac{\partial \varrho}{\partial x}$$

In the first case, the warm air has an (individual) acceleration upwards relatively to the individual air particles of the cold wedge. In the second case, the warm air has a downward acceleration relative to the air of the cold wedge. When the heaviest air mass is to the right $\frac{\partial \varrho}{\partial x}$ is always positive. g, Ω_z, and $\operatorname{tg} \Theta$ are also positive, so that the entire right side becomes positive. The quantity $\frac{\partial(\varrho v)}{\partial x}$ is a measure for the change observed in the motion tangential to the contour lines of the boundary surface when passing from the warm to the cold air. It is, as a rule, positive, and obtains its highest positive value in the case of accentuated V shaped troughs. (In the case of cold fronts moving from the west, we must again use the artifice to turn the system of co-ordinates so that the cold air appears on the right hand side. The analogy with warm front surfaces is then obvious.)

The warm front surface which we have analysed by aid of the Säntis registrations belongs to the first category. The turn of wind at the passage of the surface is so small that the term $\frac{g}{2\Omega_z} \operatorname{tg} \Theta \frac{\partial \varrho}{\partial x}$ becomes the deciding one for the acceleration. Higher up on the same surface (Zugspitze and Sonnblick) we find, however, a smaller $\frac{\partial \varrho}{\partial x}$, and we may expect that the term $\frac{g}{2\Omega_z} \operatorname{tg} \Theta \frac{\partial \varrho}{\partial x}$ at still greater heights will be overcompensated by the

term $\frac{\partial(\varrho v)}{\partial x}$. The warm air will then be accelerated downwards relatively to the air of the cold wedge, in other words, its upward sliding will gradually retard and finally stop. At what level this will take place depends on the temperature distribution in both air masses. It no doubt happens, especially in high latitudes, that the warm air particles may slide upwards the cold wedge from the ground to Ci Str level. It is, however, more frequent, especially in lower latitudes, that an air individual which starts from the ground stops the ascending motion somewhere in the «Alto» level.

The motion which characterizes the surface of subsidence — downward sliding of the warm air relatively to the air of the cold wedge — can only result when the condition

$$\frac{\partial(\varrho v)}{\partial x} > \frac{g}{2\Omega_s} \operatorname{tg} \Theta \frac{\partial \varrho}{\partial x}$$

has prevailed for a period of time. Surfaces of subsidence have usually very small inclinations, but $\frac{\partial \varrho}{\partial x}$ is often found to be very great. The downward sliding of the warm air can therefore only arise when there is a great positive $\frac{\partial(\varrho v)}{\partial x}$ at the surface. That means in practice a strong veer of wind at the passage of the surface on mountains, or in the case of an aerological ascent, a corresponding turn of wind to the right when passing from below through the surface. In fact, a distinct turn of wind in this direction is usually found at the surfaces of subsidence, as, for instance, also at that one which passed Säntis at $16^3/_4{}^h$ the 1st of February, 1913. When the turn of wind is found not to fulfill the condition

$$\frac{\partial(\varrho v)}{\partial x} > \frac{g}{2\Omega_s} \operatorname{tg} \Theta \frac{\partial \varrho}{\partial x},$$

the downward sliding of the warm air particles must be decreasing. This must, no doubt, have been the case for the surface of subsidence which passed Säntis at 12^h with very little turn of wind.

Appendix: **The Effect of Friction.**

The internal friction of the air has in this paper been neglected. According to the investigations of Hesselberg and Sverdrup*) one is entitled to do so when dealing with the motion of large air masses as in our case, for instance, the whole of the warm sector current or the whole of the cold wedge. It is, however, indispensable to consider friction in order to understand the motion of the air masses close to the boundary surface. The laws of friction are, however, still so unknown that we can only make some qualitative discussions.

---

*) Th. Hesselberg und H. U. Sverdrup: «Die Reibung in der Atmosphäre». Veröffentlichungen des Geophysikalischen Instituts der Universität Leipzig. Heft 10.

In the vicinity of an «atmospheric discontinuity» one must, no doubt, reckon with a coefficient of friction which varies from one part of the medium to another. The effective force of friction may then be represented by*):

$$R_x = \eta \frac{\partial^2 u}{\partial z^2} + \frac{\partial \eta}{\partial z}\frac{\partial u}{\partial z}$$

$$R_y = \eta \frac{\partial^2 v}{\partial z^2} + \frac{\partial \eta}{\partial z}\frac{\partial v}{\partial z}$$

or when referred to the unit of mass:

$$\frac{1}{\varrho} R_x = \frac{1}{\varrho}\left(\eta \frac{\partial^2 u}{\partial z^2} + \frac{\partial \eta}{\partial z}\frac{\partial u}{\partial z}\right)$$

$$\frac{1}{\varrho} R_y = \frac{1}{\varrho}\left(\eta \frac{\partial^2 v}{\partial z^2} + \frac{\partial \eta}{\partial z}\frac{\partial v}{\partial z}\right)$$

The first term $\frac{\partial^2}{\partial z^2}$ is negative where the wind component in question has its maxima, and positive where it has its minima of velocity. The effect of friction is thus in the first place to smoothen out the extreme velocities. In our case it would mean that the foremost part of the rapidly moving warm current should be retarded and the neighbouring part of the cold air accelerated, with the effect that the wind contrast at the boundary surface becomes less abrupt.

The second term $\frac{\partial \eta}{\partial z}\frac{\partial}{\partial z}$ may, however, bring important modifications at places where η varies rapidly with height. As far as I know, one has not yet found an exact formula for η as a function of other meteorological elements. It is, however, certain that η is intimately dependent on the vertical stability of the air in the manner that great stability gives a small value for η, and vice versa. By stability is then meant the expression $E = \frac{\gamma_a - \gamma}{\vartheta}$, where γ is the lapse rate of temperature in degrees per unit vertical distance, and γ_a the lapse rate of an air mass ascending adiabatically (moist adiabatic or dry adiabatic, according to the conditions)**).

Without assuming anything concerning the absolute values of η, we may expect that it will be a funktion similar to that of $\frac{1}{E}$. On Fig. 13 this quantity $\frac{1}{E} = \frac{\vartheta}{\gamma_a - \gamma}$ has been constructed as a function of z.

Starting from the left we have the temperature-height diagram as it must have been according to the Säntis thermogram. The next curve represents the lapse rate of temperature γ in degrees per metre vertical distance. We see that the cold wedge has a normal lapse rate of about $-0.7°/100$ m. In the transitional zone the lapse rate is smaller, and for a time it surpasses the zero value (inversion of temperature). In the warm sector the lapse rate again gradually approaches a normal value of about $0.6°/100$ m. Although the air does not ascend in the whole of the zone of mixing, we may assume that the ascending current above contains enough water (snow) in condensed form to keep the whole air mixture saturated. We shall therefore reckon with moist adiabatic

*) l. c. p. 286.

**) See Hesselberg, Th.: «Über die Stabilitätsverhältnisse bei vertikalen Verschiebungen in der Atmosphäre und im Meer». Ann. d. Hydrographie und Maritimen Meteorologie, 1918, p. 118.

processes not only in the ascending part of the warm air, but also through the whole zone of mixing. Under this supposition the curve for $\gamma_a - \gamma$ is derived. It contains two discontinuities, one at the bottom of the zone of mixing and one at the upper limitation of the cloud layer. These discontinuities appear still more distinct in the curve for $\frac{1}{E} = \frac{\vartheta}{\gamma_a - \gamma}$, especially the lowest one at which the value of $\frac{1}{E}$ suddenly increases to ∞. (This latter discontinuity of stability also appears very distinctly in the registration of wind direction on Fig. 5.) In a thin layer in the lowest part of the zone of mixing, we may

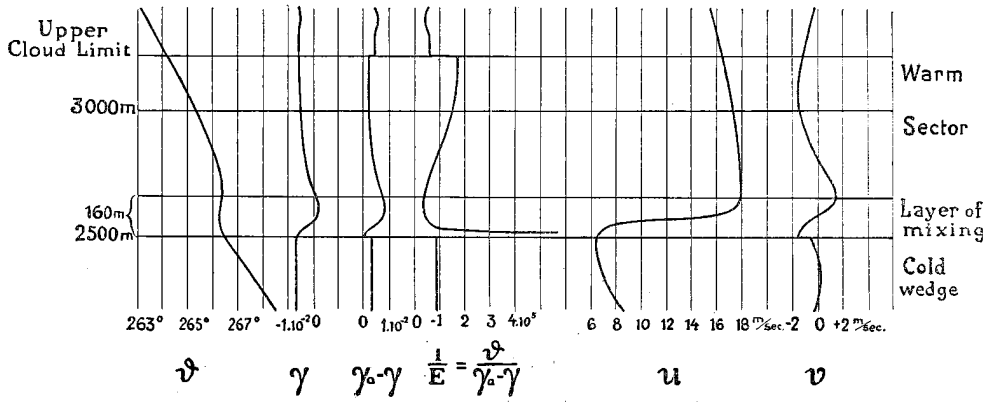

Fig. 13. Stability of the air at the warm front surface.

thus expect to have a very great coefficient of internal friction. The remaining part of this zone has, however, a very stable stratification and probably a small internal friction.

Basing upon the curves for $\frac{1}{E}$ and those for u and v, we may now find in what manner the term $\frac{\partial \eta}{\partial z}\frac{\partial}{\partial z}$ will act.

For $\frac{\partial \eta}{\partial z}\frac{\partial u}{\partial z}$ we find:

In the cold wedge: no effect, as $\frac{\partial \eta}{\partial z}$ is very small.

Just at the entrance into the layer of mixing: $\frac{\partial \eta}{\partial z}$ infinitely great positive but $\frac{\partial u}{\partial z}$ zero. Effect to the term $\frac{\partial \eta}{\partial z}\frac{\partial u}{\partial z}$ indeterminate.

The lowest 100 metres of the layer of mixing: $\frac{\partial \eta}{\partial z}$ great negative and $\frac{\partial u}{\partial z}$ great positive, the product great negative, that is: *the force directed against the wind.*

In the upper part of the layer of mixing: $\frac{\partial \eta}{\partial z}\frac{\partial u}{\partial z}$ very small positive, i. e., *the force directed with the wind.*

In the warm current: $\frac{\partial \eta}{\partial z}\frac{\partial u}{\partial z}$ moderate negative.

We thus see that the frictional effect represented by the term $\eta \frac{\partial^2 u}{\partial z^2}$ will be modified by the term $\frac{\partial \eta}{\partial z}\frac{\partial u}{\partial z}$. While the first term gave acceleration at the minima and retardation

at the maxima of velocity, the second term gives a strong component of retardation in the lowest part of the layer of mixing and relatively small effects elsewhere. The part of the force of friction which depends upon $\frac{\partial \eta}{\partial z}\frac{\partial u}{\partial z}$ will thus tend to maintain the contrast of velocities from the lowest to the uppermost part of the layer of mixing. It thus depends on the relative magnitude of the terms $\eta \frac{\partial^2 u}{\partial z^2}$ and $\frac{\partial \eta}{\partial z}\frac{\partial u}{\partial z}$ (and of course also of the forces represented in Fig. 8) whether the abruptness in the transition of wind velocity from the cold to the warm mass shall increase or decrease.

The analogous discussion of the term $\frac{\partial \eta}{\partial z}\frac{\partial v}{\partial z}$ gives the following result:

In an infinitely thin sheet at the lowest boundary of the layer of mixing: $\frac{\partial \eta}{\partial z}$ infinitely great positive and $\frac{\partial v}{\partial z}$ infinitely great negative. The product infinitely great negative.

The negative sign of $\frac{\partial \eta}{\partial z}\frac{\partial v}{\partial z}$ is maintained throughout the lowest 100 metres of the layer of mixing $\left(\frac{\partial \eta}{\partial z}\right.$ negative and $\left.\frac{\partial v}{\partial z}\right.$ positive$\Big)$.

In the uppermost 60 metres of the layer of mixing the product is small positive. Still higher negative again, and so on.

The important result is that there is a *great difference between the value of* $\frac{\partial \eta}{\partial z}\frac{\partial v}{\partial z}$ *at the uppermost and the lowest part of the layer of mixing.* This difference acts in the same manner as found for the other component, namely that it tends to maintain the observed difference of wind.

At the top of the cloud layer the discontinuity of stability ought to have analogous effects on the wind distribution as found underneath. This part of the wind registration is, however, in our case disturbed too much by turbulence (see Fig. 5) so as to allow any analysis of details.

It would be an interesting field of investigation to study the friction at the surfaces of discontinuity by aid of the registrations from mountain observatories. For this special purpose it would, however, be indispensable to have an anemograph registering wind velocity directly. Only with such an instrument would one get the exact structure of the wind field, the analysis of which could inform us concerning the nature of the force of friction.

The above discussion on the force of friction at an atmospheric boundary surface is therefore only a first attempt to get an orientation. At all events it is evident, that friction will only modify details, without changing the main results arrived at in this paper.

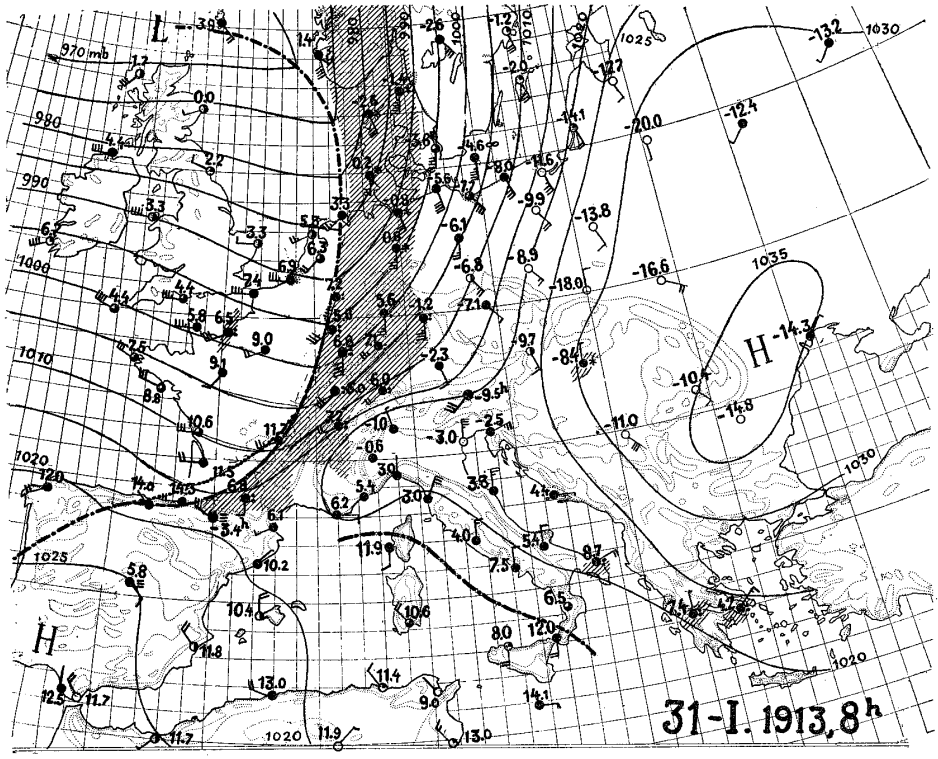
31-I. 1913, 8h

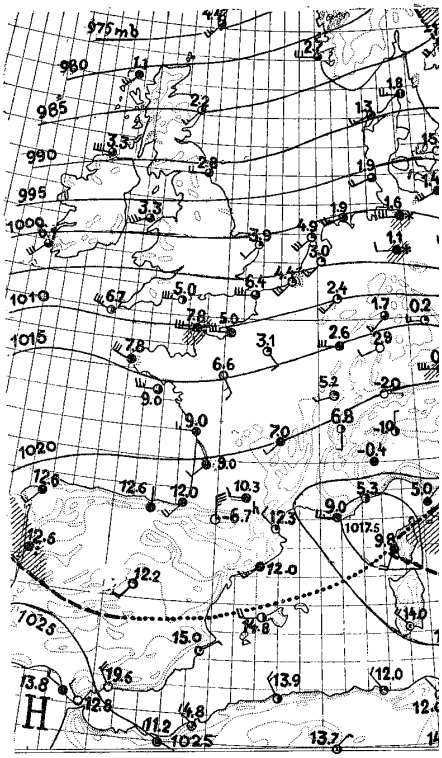

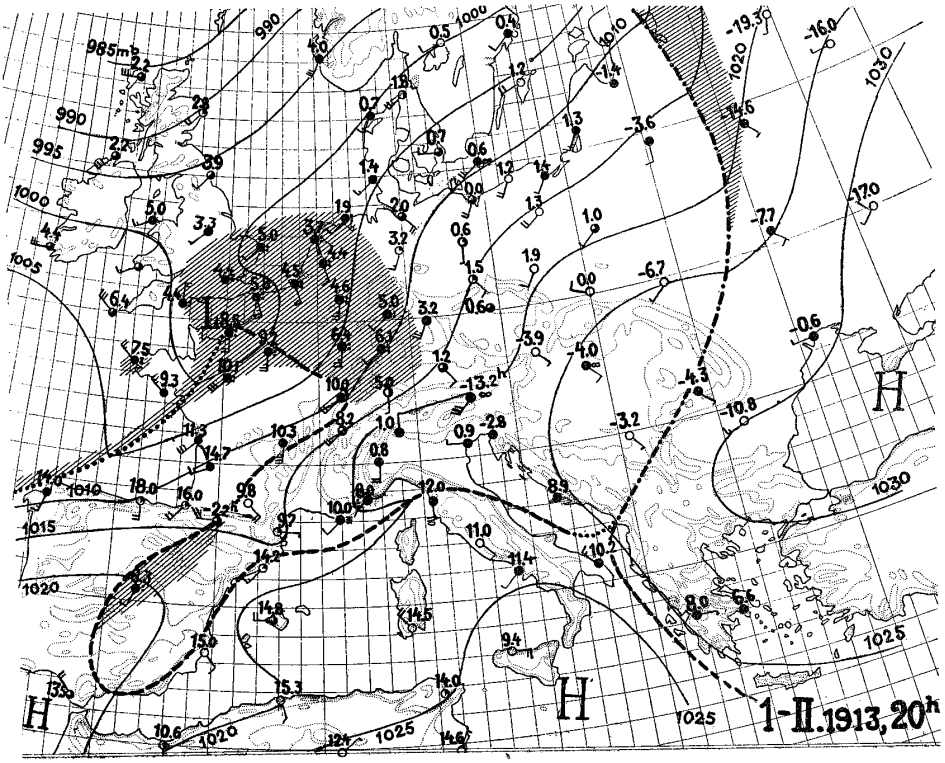
1-II. 1913, 20h

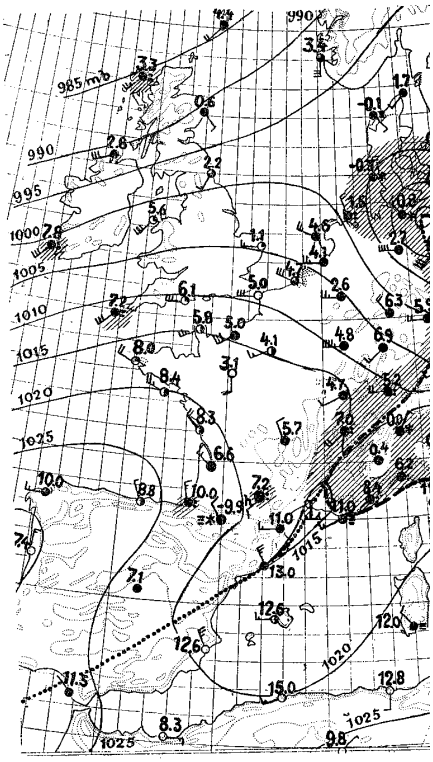

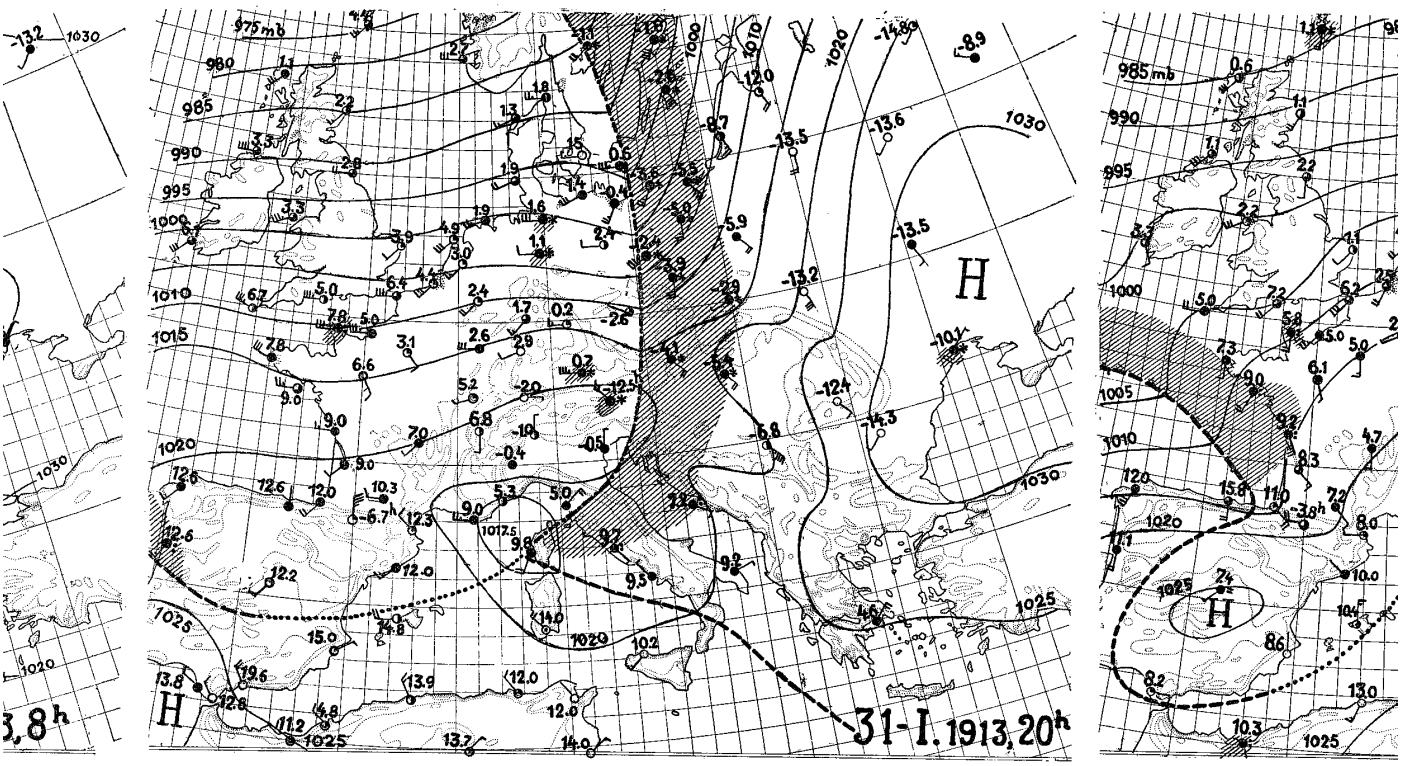
31-I. 1913, 20h
H
975 mb
985 mb
990
995
1000
1005
1010
1015
1020
1025
1030

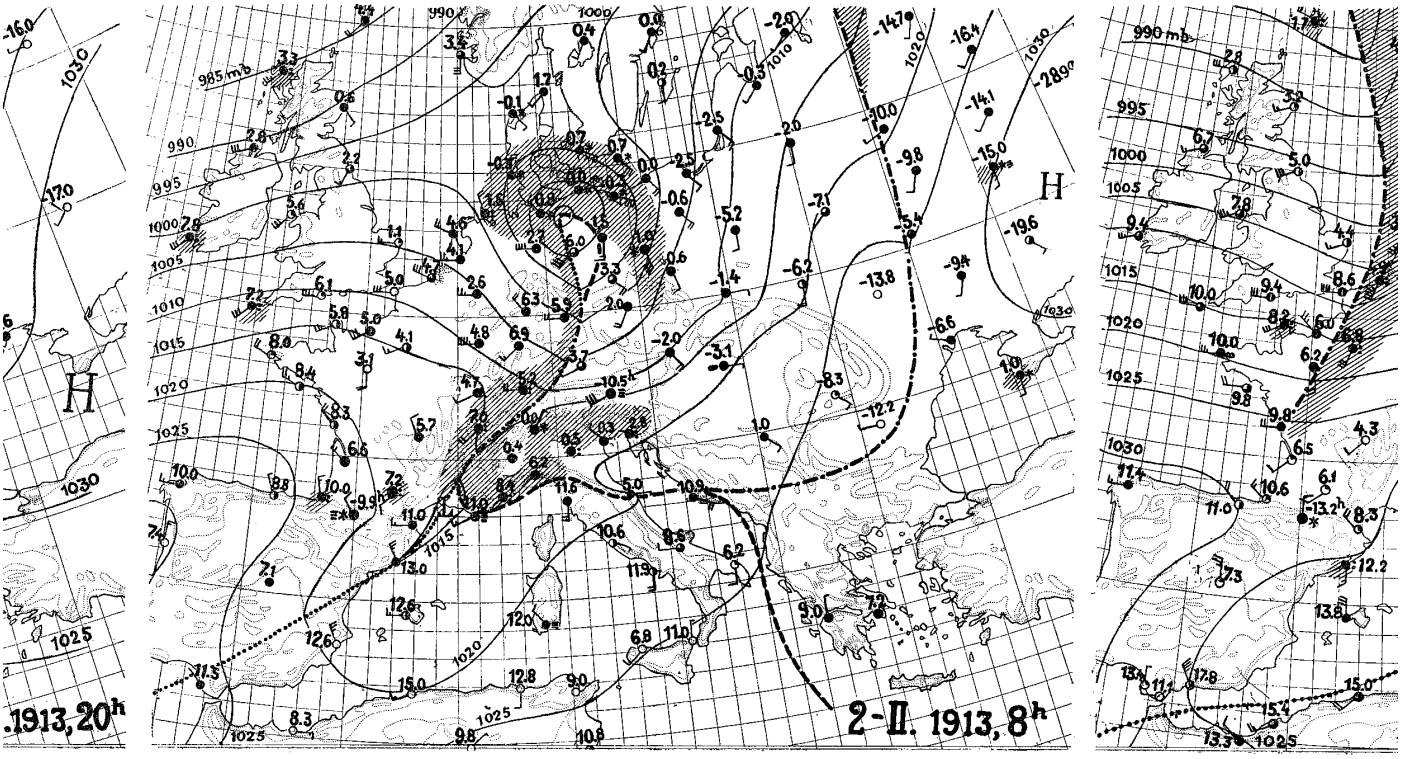
2-II. 1913, 8h
H
990 mb
985 mb
995
1000
1005
1010
1015
1020
1025
1030

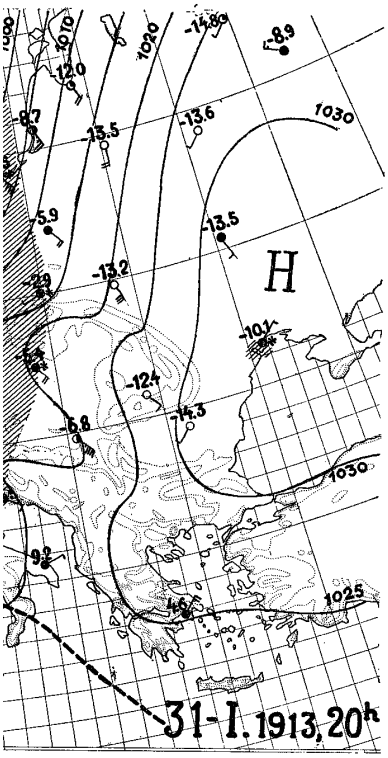
H
1030
1025
31-I. 1913, 20h

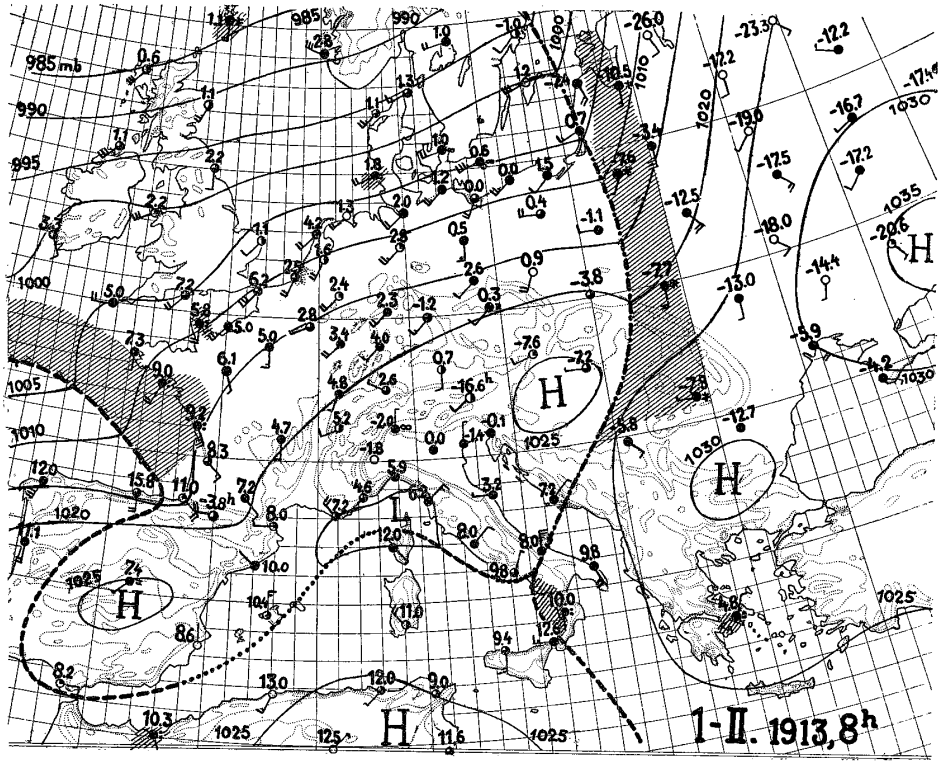
985 mb
990
995
1000
1005
1010
1020
1025
1030
H
L
1-II. 1913, 8h

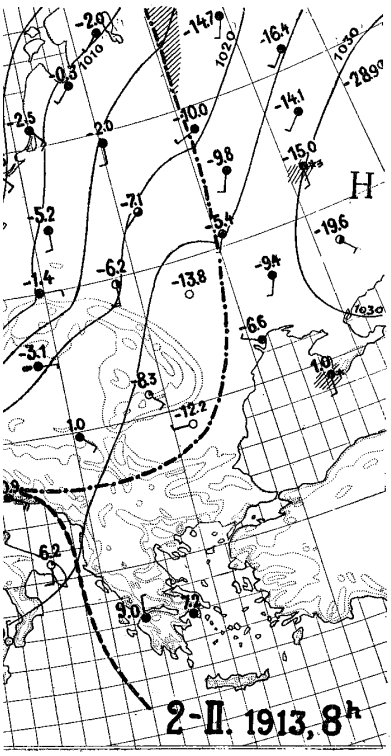
1010
1020
1030
H
2-II. 1913, 8h

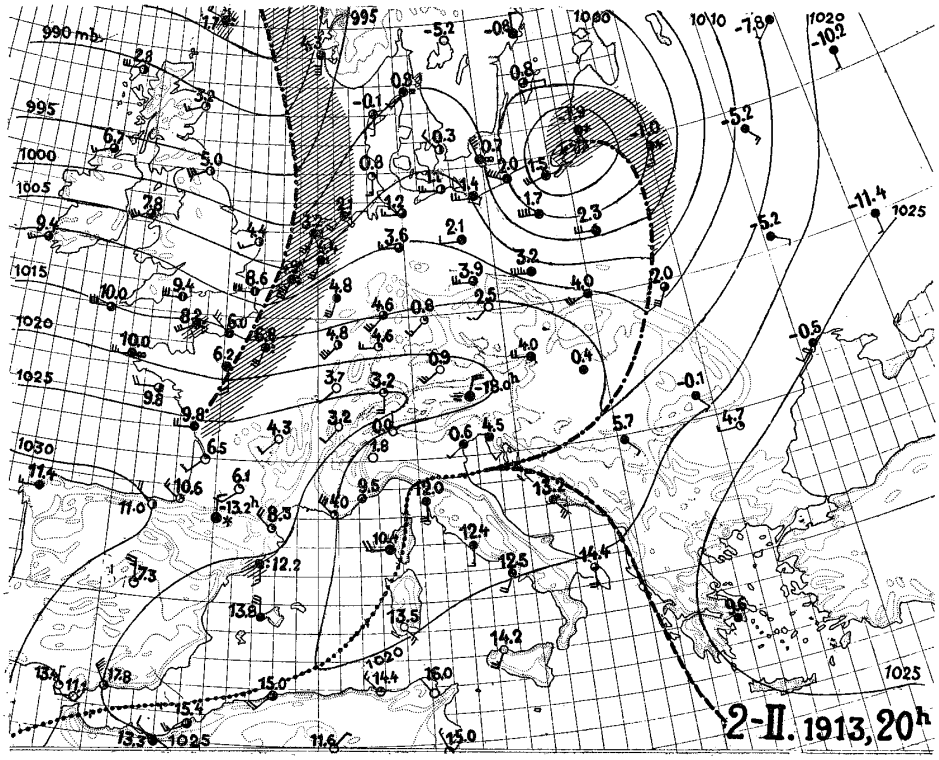
990 mb
995
1000
1005
1015
1020
1025
1030
1020
1025
2-II. 1913, 20h